Effect of density-dependent individual movement on emerging spatial population distribution: Brownian motion vs Levy flights

John Ellis[a], Natalia Petrovskaya[a1] and Sergei Petrovskii[b]

[a] School of Mathematics, University of Birmingham, Birmingham, UK.

[b] Department of Mathematics, University of Leicester, Leicester, UK.

Abstract

Individual animal movement has been a focus of intense research and considerable controversy over the last two decades, however the understanding of wider ecological implications of various movement behaviours is lacking. In this paper, we consider this issue in the context of pattern formation. Using an individual-based modelling approach and computer simulations, we first show that density dependence ("auto-taxis") of the individual movement in a population of random walkers typically results in the formation of a strongly heterogeneous population distribution consisting of clearly defined animals clusters or patches. We then show that, when the movement takes place in a large spatial domain, the properties of the clusters are significantly different in the populations of Brownian and non-Brownian walkers. Whilst clusters tend to be stable in the case of Brownian motion, in the population of Levy walkers clusters are dynamical so that the number of clusters fluctuates in the course of time. We also show that the population dynamics of non-Brownian walkers exhibits two different time scales: a short time scale of the relaxation of the initial condition and a long time scale when one type of dynamics is replaced by another. Finally, we show that the distribution of sample values in the populations of Brownian and non-Brownian walkers is significantly different.

Keywords: animal movement, individual-based modelling, density-dependence, pattern formation, long transients

[1]Corresponding author. Email: n.b.petrovskaya@bham.ac.uk

1 Introduction

Spatial distributions of ecological populations are rarely uniform. Distinctly heterogeneous or even 'patchy' distributions are ubiquitous in different ecosystems and are seen at different spatial and temporal scales [44, 45]. This phenomenon—also referred to as aggregation or patchiness [18, 44] or, more generally, ecological pattern formation [59]—is known to have important implications for population dynamics [55, 66, 87], nature conservation and renewable resource management [16, 92, 93], agriculture and forestry [1, 39, 75, 81, 90], monitoring and pest control [62, 64, 67], etc. Correspondingly, the factors and processes resulting in ecological pattern formation have been a focus of substantial empirical and theoretical research for a few decades. Several mechanisms have been identified that can result in a heterogeneous spatial population distribution [51, 52] (see also [65] for a brief review). Pattern formation on large (landscape or regional) spatial scales usually occurs on a multi-annual or multi-generational time scale as the corresponding mechanisms involve the population growth. Large scale patterns are often attributed to the interplay between dispersal and the inter-specific interactions [43] such as the interaction of a given species with its predator or its prey [51, 52] or more generally with a resource that limits its population growth, e.g. water in case of vegetation patterns [40, 42]. Alternatively, large scale patterns can arise from the effect of spatially correlated external factors [50] that may result in synchronization between disconnected habitats [32, 47, 73]. In a more general case, large scale patterns emerge as a result of a combined effect of the population growth, dispersal and environmental noise [7].

Meanwhile, a distinctly heterogeneous population distribution is also often seen on a much smaller, 'within generation' time scale where population reproduction is not directly involved, and on a much smaller spatial scale, e.g. within a given forest, lake, meadow or farm field where animals of a given species are aggregated or grouped together to create flocks, swarms, herds etc. [41, 58] or simply well-defined patches of the population density [1, 56, 63]. Unless it can be attributed to a distinct environmental heterogeneity (e.g. animal grouping at a better feeding ground), this phenomenon is thought to be either a consequence of animal 'sociality' [17, 23] or the effect of the density-dependence of the movement [48, 85]. The specific animal's reaction can be of somewhat different type. In the former case, the animal adjusts its movement velocity to those of the animals around, hence resulting in a collective movement as is often seen in swarms, flocks and herds [23, 41]. In the latter case, the animal's movement direction correlates with the direction of the population density gradient. Although the movement speed of different animals is not necessarily correlated in this case, the movement direction of a given animal tends to be towards areas with higher population density; the phenomenon that is known as taxis [38, 53, 85, 86]. We mention here that these two types are not exhaustive and more complicated types of density dependence can happen too [31].

In either of the above cases, the small-scale, within-generation patterns in the spatial population distribution emerge as a result of a response of individual animals to the presence of their conspecifics; hence, the properties of individual animal movement are at the core of it [84]. However, the specific dynamical mechanisms often remain obscure. Over the last two decades, there has been an intense debate on the issue of individual animal movement.

Traditional approaches used to regard it as a Brownian motion [35, 77] where the dispersal kernel decays with the distance very fast (exponential or faster) and hence the probability of long-distance travel is suppressed. More recently, there was a trend to associate animal movement with Levy flights [71, 79, 88]: the movement type with a much higher probability of long-distance travel described by a 'fat-tailed' dispersal kernel (e.g. power law) [89]. Whilst details of this debate are outside of the scope of this paper, one aspect that has been almost completely overlooked so far (but see [68]) is the ecological consequences of the movement behaviour on the population level. Our study aims to bridge this gap by investigating the effect of various types of the individual movement on the pattern formation.

In this paper, we consider a mechanistic individual-based model that relates the formation of a patchy spatial distribution of the population abundance to the density-dependent individual animal movement. We first consider the case where the animals perform Brownian motion (i.e. are described by a Gaussian dispersal kernel, the normal distribution) and show that the density dependence of the movement leads to formation of distinct animals groups or clusters. We then consider the case of animals performing non-Browninan motion (described by a power law kernel) to show that, in combination with the density dependence, it leads to pattern formation with different properties. For a power law kernel, the population tends to be less aggregated than for an equivalent Gaussian kernel and the clusters (patches) appear to be less stable, in particular allowing for dynamical transition between different states. The distribution of sample values is shown to be essentially different too.

2 Model

In order to simulate animal movement with different properties and its effect on the emerging spatial population distribution, we use the individual-based modelling approach [11, 22, 33, 84]. Correspondingly, the position of each individual animal is described explicitly at some designated moments of time, $t_k,\ k = 0, 1, \ldots, t_{k+1} = t_k + \Delta t$ where Δt is the time increment. In a general case, Δt can vary with time. In this paper, we consider it to be constant, $\Delta t = 1$; therefore, $\{t_k\}$ is a set of positive integers.

We restrict our study to a system with one spatial dimension (1D). In terms of a more realistic movement of animals walking or crawling on the surface, e.g. (x, y) plane, this may correspond to either a transect across the habitat or to a narrow stripe, so that we are only concerned with the x coordinate of the animals but not with their y coordinate. Extension of our results onto a 2D system will be briefly discussed in Section 4.

Let us consider a population of N animals. Given the location of the nth animal is known at time t, its position at the next moment $(t + 1)$ is simulated as

$$x_n(t + 1) = x_n(t) + \Delta x, \tag{1}$$

where the increment Δx thus gives the size of a 'step' made by the animal along its movement path during the time increment $\Delta t = 1$. The movement starts from some initial location, $x_n(0) = x_{n,0}$.

Once sufficient information about Δx is available, the movement process is fully defined. Following [14, 33, 84], we consider Δx to be a random variable distributed according to a certain probability density function $\rho(\Delta x)$. We refer to function $\rho(\Delta x)$ as the dispersal kernel. For the sake of simplicity, we assume that all animals have identical movement behaviour so that function ρ is the same for all animals.

We mention here that the randomness of the movement step is a subtle and somewhat controversial issue. It is more likely to reflect the incompleteness of the available information about the complex process of animal's decision-making rather than the randomness in the strict sense (for a detailed discussion of the "bugbear of randomness", see [84]). However, the theoretical framework describing individual animal movement as a random walk, at least on certain spatial and temporal scales, has been shown to be in a very good agreement with empirical studies and is widely accepted as an adequate research setup [6, 14, 36, 84, 89].

Since the main purpose of this study is to reveal possible population-level consequences of different patterns of individual movement (in particular, Brownian and non-Brownian motion), we consider two qualitatively different cases. In the first case, the dispersal kernel is a normal distribution with the zero mean and the variance σ^2:

$$\rho\left(\Delta x\right) = \rho_G\left(\Delta x|0,\sigma^2\right) = \frac{1}{\sqrt{2\pi\sigma^2}}\exp\left(-\frac{(\Delta x)^2}{2\sigma^2}\right). \tag{2}$$

We will refer to animals performing the movement described by (2) as Brownian walkers.

In the second case, the dispersal kernel is described by a power law using the following parametrization [27]:

$$\rho\left(\Delta x\right) = \rho_P\left(\Delta x|k,\gamma\right) = \frac{C}{(k+|\Delta x|)^\gamma}, \tag{3}$$

where $k > 0$ and $\gamma > 1$ are parameters of the distribution and $C = 0.5(\gamma-1)k^{\gamma-1}$ is the normalizing coefficient to ensure that the total probability is one, i.e. $\int_{-\infty}^{\infty}\rho(\xi)d\xi = 1$. Note that parameter k has the dimension of length, hence it has the meaning of a characteristic distance of the movement process (cf. Section 3 in [37]). For $\gamma \leq 3$, the stochastic movement described by Eq. (3) is often referred to as Levy flight[2]. For convenience, we will refer to animals performing the movement described by dispersal kernel (3) as non-Brownian walkers, and in the particular case $1 < \gamma \leq 3$ as Levy walkers. Asymptotically, i.e. for large Δx, the dispersal kernel (3) coincides with the Lomax distribution [49] which is a special case of Pareto distribution Type II [4]. We mention here that, being originally introduced as a model to describe the distribution of wealth in the society [60], Pareto distributions were later used to describe a broad range of phenomena in natural sciences, including animal movement [89].

We consider the movement in a closed domain so that, for any n, $0 < x_n(t) < L$ at any t. The closed boundaries at $x = 0$ and $x = L$ are modelled by introducing an additional rule. Let the value of Δx generated for the $(n+1)$th step be such that either $x_n(t+1) < 0$ or $x_n(t+1) > L$. Then this value of Δx is aborted, hence effectively changing the animal's

[2]In ecological literature, it is sometimes also referred to as a Levy walk, which is not entirely correct as the Levy walk is a different stochastic process, e.g. see [89].

decision to leave, and a new Δx is generated to make sure that the animal remains inside the domain, i.e. $0 < x_n(t+1) < L$.

2.1 Density-dependent movement

In the simulation procedure described above, all animals move independently, i.e. the presence of their conspecifics in a vicinity of their location does not have any effect on their choice of the next movement step. As is mentioned in the introduction, this is not always true. A moving animal often reacts to the presence of other animals, i.e. by correlating the direction of its movement with the population density gradient, so that the individual movement becomes density dependent.

In order to account for the taxis-type density dependence, we need to modify the individual-based modelling approach. Firstly, we introduce the 'perception radius' $R \geq 0$ [69, 78]. This is the distance in each direction (in the 1D case, left or right) over which an animal can detect the presence of other animals. At any moment t, only those animals that are within the region $[x_n(t) - R, x_n(t) + R]$ are taken into account and hence can affect the movement. Note that if $R = 0$, then there is no density dependence and the animals will perform unbiased random movement, cf. Eqs. (1–2).

Secondly, we introduce a parameter P to quantify the strength of the directional bias, $0 \leq P \leq 1$. Let n_l and n_r be the total number of animals that are counted (within the perception radius), respectively, to the left and right of the given animal. Let u be an auxiliary random variable uniformly distributed over interval Ω where Ω is defined as follows:

$$\Omega = [P-1, P] \ \text{ if } \ n_l < n_r, \qquad \Omega = [-P, 1-P] \ \text{ if } \ n_l > n_r, \tag{4}$$

$$\Omega = [-0.5, 0.5] \ \text{ if } \ n_l = n_r.$$

In general, the absolute value of the movement step of the density-dependent movement and its direction are affected by different factors; hence, we consider them to be uncorrelated. Thus, they can be regarded as mutually independent random variables. The probability density of having the movement step of a given value, say Δx_d, is then given by a product of the probability density of making a step of a given length $|\Delta x|$ and the probability of moving left or right. Therefore, any realization of this random variable can be written as

$$\Delta x_d \ = \ \text{sign}(u) \cdot |\Delta x|, \tag{5}$$

where Δx is the movement step of the unbiased (density-independent) movement, e.g. as given by (2) or (3).

If $P = 1$, then the animal always moves along the gradient of the population density. For $P = 0.5$, the probability of u being positive or negative is exactly 0.5, so that the movement becomes unbiased (effectively, density-independent). Values of $P < 0.5$ correspond to a negative density-dependence where the animal is more likely to move against the gradient (towards the area with lower population density); we do not consider this case here. In the simulations below, we consider $0.5 < P < 1$. Note that, in this case, a given animal does

not move deterministically left or right simply depending on whether $n_l > n_r$ or $n_l < n_r$. In order to account for the complexity of movement decisions, we therefore have assumed that a certain degree of randomness is always present, i.e. the animal can with some probability move against the gradient of the population density, not necessarily along the gradient (as is expected on average).

In order to make the model complete, we need to specify what happens if a given animal meets another animal during its movement step, i.e. if its final position after the step is behind another animal. In this paper, we consider the rule that the moving animal does not stop until it reaches its final destination, i.e. its movement step is not terminated if it comes close to another animal. (Alternatives to this rule will be discussed in Section 4.) Note that it does not mean that the animal has to jump other each other: here we recall that our 1D model corresponds to a narrow stripe rather than a line, so passing-by is possible.

Sample trajectories generated by the above rules are shown in Fig. 1 (obtained for $P = 0.75$ and $R = L$, i.e. in the case of a global coupling where each animal can see all other animals). It is readily seen that, as a result of the density-dependent movement, the animals tend to group together to form a 'cluster'. This observation agrees with intuitive expectations and, by itself, is hardly surprising. What is not intuitive is the properties of the arising spatial pattern (e.g. how many clusters can emerge) and how they depend on the movement parameters P, R and σ (or γ and k). We address this question in the next section.

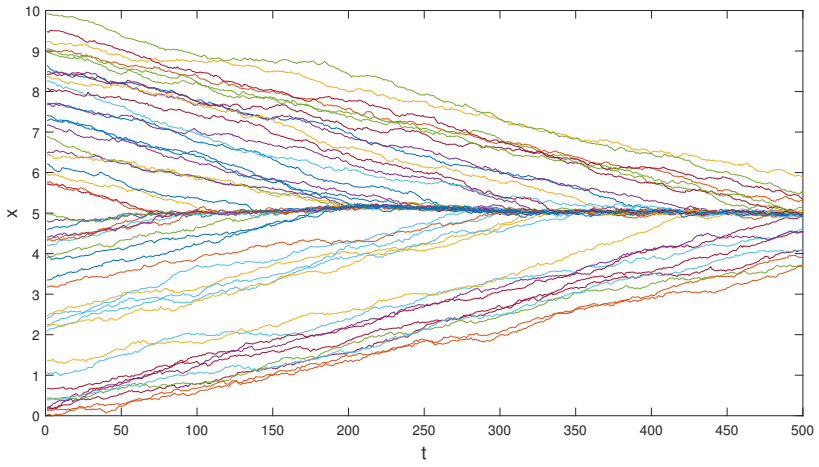

Figure 1: Individual movement paths of 50 insects over 500 time steps in the case of density-dependent movement with P=0.75 and $R = 10$ generated by the density-dependent random walk model using Gaussian dispersal kernel (2) with $\sigma = 0.02$. Each insect is represented by a different colour. At time $t = 0$, the population is randomly distributed over the domain $0 \leq x \leq 10$ with constant probability density.

Since our focus is on the dispersal of the population rather than individuals, it is more convenient to describe the population distribution over space by the population density rather than by an array of the coordinates for all individuals. In order to calculate the population density, we split the domain to a number of 'bins'; the number of animals inside a given bin

divided by the length of the bin will approximate the population density at the location of the bin. The distribution of the population density over space then takes the form of a histogram.

Now, since the purpose of this study is to analyze the dynamics of the population clusters (patches) as a function of the movement parameters, we need a formal definition of the cluster. We say that a group of adjacent bins forms a cluster if:

1. for a given parameter $0 < b < 1$, there is a bin in the group ('major bin') that contains a proportion of the total number of animals that is larger than b;

2. any bin on either side of the 'major bin' belong to the given cluster if it contains the number of animals larger than 0.2% of the total number.

3 Simulation results

Our goal is to reveal typical properties of the emerging spatial population distribution in the population of animals performing density-dependent individual random movement (as described in the previous section) subject to the properties of the dispersal kernel (Gaussian or power law, see Eqs. (2–3)) and the strength of the density-dependence as given by parameters P and R. For the initial condition, we consider that the population is distributed uniformly (in the statistical sense) over the domain. Mathematically, it means that the initial location of each individual is generated using the probability density function $\rho_0(x)$ that does not depend on space; for a 1D domain of length L, $\rho_0 = 1/L = const$. An example of the initial population distribution is shown in Fig. 2. Note that, due to the random nature of the initial distribution, the exact profile changes with each new simulation run. Here and below (unless

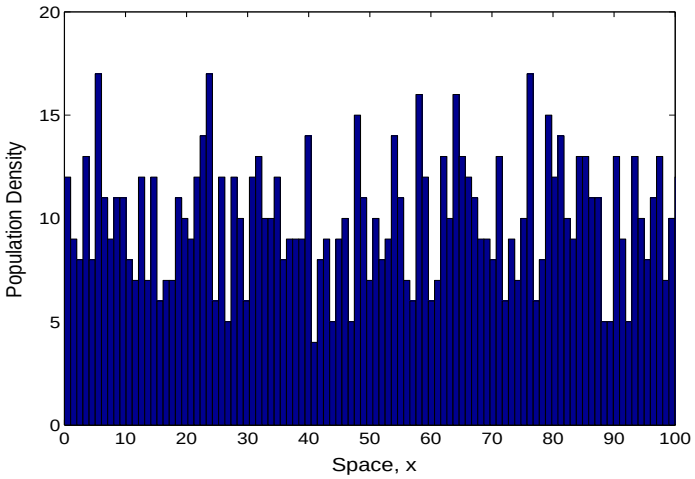

Figure 2: Example of the initial distribution. The total number of $N = 1000$ animals is distributed uniformly (in the statistical sense, i.e. with constant probability density) over the domain of length $L = 10$. The domain is split into one hundred bins of equal size $\Delta x = 0.1$; the horizontal axis shows the bin number, so that the corresponding coordinate $x = 0.1 \times$bin number. Each column shows the number of animals in a given bin.

explicitly stated otherwise), we consider the population of $N = 1000$ animals moving in the domain of length $L = 10$ (in abstract units). The domain is split into one hundred bins, so that the spatial width of each domain is 0.1. For the proportion defining the boundaries of the cluster, the value $b = 0.02$ is used (i.e. 2% of the total population).

We mention here that our choice of parameters here and below is largely hypothetical. The goal of this paper is to make an insight into some generic properties of the population dynamics rather than to analyse the dynamics of a specific population. It is not our purpose here to compare the simulation results to real field or laboratory data obtained for a real animal species. Looking for 'true' parameter values is therefore hardly necessary, if possible at all, given the schematic nature of our model. Instead, our purpose is to reveal the difference between the spatiotemporal patterns emerging for the two different movement types and between the systems properties arising in different parameter ranges (i.e. 'small' vs 'large', and/or to establish what is 'small' and what is 'large') with a particular focus on understanding the effect of the directional bias as quantified by the parameter P.

3.1 Normal distribution: Brownian walkers

We begin with the case where the dispersal kernel is given by a normal distribution; see Eq. (2). We consider animal movement in a large spatial domain, so that the characteristic movement step is much less than the domain size, $\sigma/L \ll 1$ (this condition will be relaxed in Section 3.3). Typical simulation results are shown in Fig. 3. It is readily seen that the evolution of the initial population distribution due to the individual density-dependent movement results in the aggregation of the population into several clusters or patches. The population density (i.e. the number of animals per bin) is high in the center of the cluster but close to zero between the clusters.

Apparently, there is not much difference between the population distributions shown in the left and right panels of the last row of Fig. 3, which corresponds to a large time. The question is whether the system evolves to a stationary spatial distribution and, if yes, what is the characteristic time scale for the convergence to the steady state. In order to make an insight into these matters, for each cluster we calculate its size (the total number of animals in the cluster) and its width (the distance between the left-most and right-most bins in the cluster). Figure 4 shows the size and width of the four clusters shown in Fig. 3 vs time. It is readily seen that the system never reaches the steady state in a strict sense as some random fluctuations around the steady state persist at all times, albeit being relatively small. The time required for the convergence to the quasi-steady state dynamics appears to depend on the size of the cluster; the larger the cluster, the longer the convergence time is. This is seen particularly well in Fig. 4b. Whilst for the smallest cluster (cluster 4) its width approaches its steady state value (up to small random fluctuations) at $t \approx 300$, for the largest cluster (cluster 1) it does not happen until $t \approx 700$. Interestingly, the convergence occurs at a somewhat different rate for the size of the cluster and for its width. For the two smallest clusters, i.e. cluster 2 and cluster 4, their size stabilizes already at $t \approx 150$ (see Fig. 4a) but their width does not reach its 'final' value until $t \approx 300$ and $t \approx 400$, respectively (Fig. 4b). For the intermediate cluster

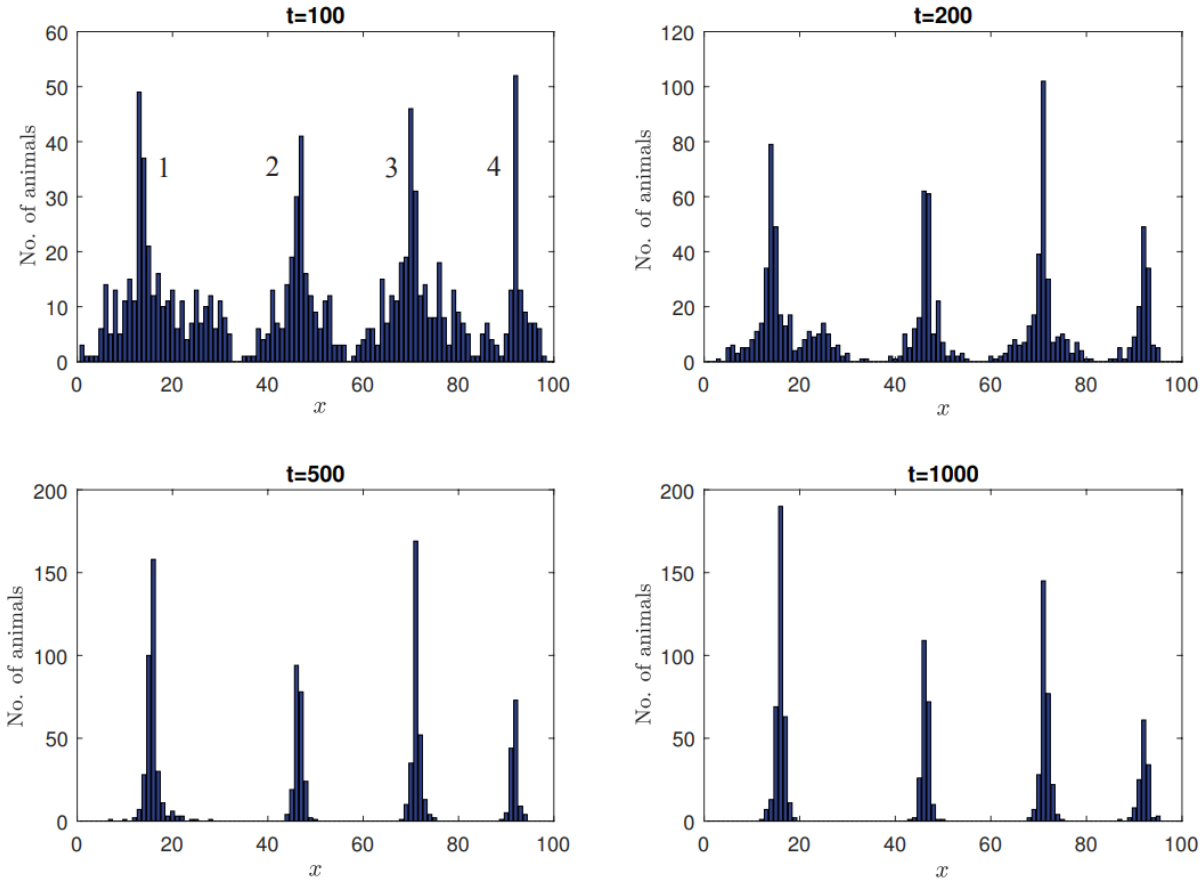

Figure 3: Population density over space at different moments of time emerging from a random-uniform initial distribution, cf. Fig. 2. Each column shows the number of animals in a given bin. Movement parameters are $\sigma = 0.02, P = 0.6$ and $R = 1$, other parameters are the same as in Fig. 2. For the convenience of a further discussion, clusters are numbered, 1 to 4, left to right; see panel (a).

3, its size stabilizes at $t \approx 250$ and its width at $t \approx 550$.

Based on the simulation results (note that Fig. 3 shows only one typical example from a large number of simulations performed) we conclude that the random-uniform initial distribution in the course of time evolves to the formation of clearly defined clusters. Interestingly, for the same parameter values the number of clusters emerging in the large time limit is not always the same. This is obviously a result of the inherent randomness of the system's dynamics which is rooted in the randomness of the individual animal movement. As just one example, Fig. 5 (obtained for the same parameters as Fig. 3) shows the evolution of the initial distribution that results in five clusters instead of four. Thus, for a given value of the movement parameters, the pattern formation in the course of the system's dynamics is described by the probabilities (frequencies) of observing a distribution with a different number of clusters (see Tables 1–3 below).

The number of clusters (more precisely, the distribution of the probabilities for each number of clusters) is different depending on the movement parameters. Figure 6 shows the population distribution over space obtained in case the perception radius is $R = 2$, other parameters and

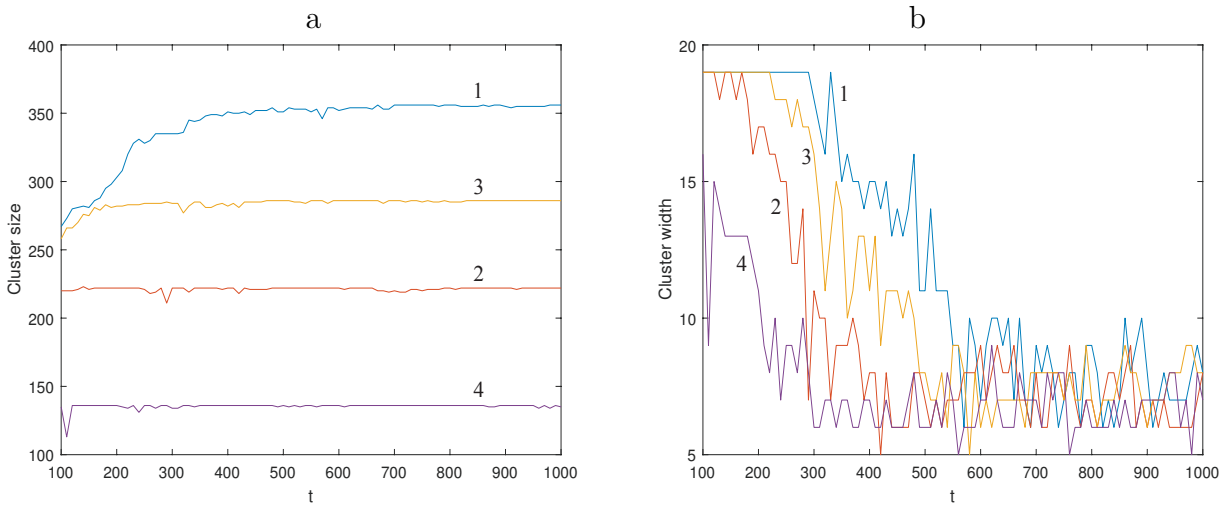

Figure 4: The cluster size and width over time, (a) and (b) respectively, for the population dynamics shown in Fig. 3. The parameters are the same as in Fig. 3. The curve numbering in panel (a) corresponds to cluster numbering in Fig. 3; note that the relative order of the curves is different from Fig. 3.

the initial distribution being the same as in Fig. 3. Obviously, in this case only two clusters are formed.

Now we investigate how the frequency of different cluster numbers depends on the movement parameters such the perception radius R, the directional bias P and the standard deviation of the dispersal kernel σ. This question has been addressed through extensive numerical simulations. For a given parameter set, one hundred simulations were run, each of them until $t = 3000$. For each of the thus obtained one hundred spatial population distributions, the

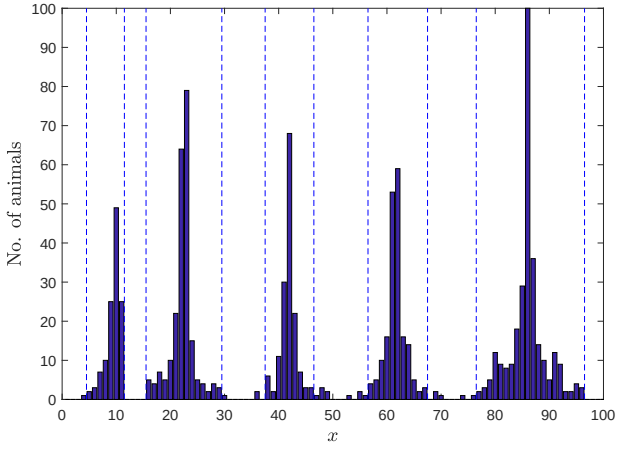

Figure 5: Population density over space obtained at $t = 200$ at a different realization (i.e. a different simulation run) of the system. Parameters are the same as in Fig. 3. The dashed vertical lines show the clusters' boundaries. The different number of clusters, i.e. five instead of four, is the result of the inherent stochasticity of the dynamics.

Table 1: The probability for different numbers of clusters obtained in simulations for different values of the perception radius R. Other parameters are $P = 0.6$ and $\sigma = 0.02$. For any given parameter set, the probabilities were calculated based on one hundred simulation runs.

No. of clusters	$R = 1$	$R = 2$	$R = 3$	$R = 4$	$R = 5$
1	0	0	0.33	1	1
2	0	0.69	0.67	0	0
3	0.03	0.31	0	0	0
4	0.53	0	0	0	0
5	0.41	0	0	0	0
6	0.03	0	0	0	0

Table 2: The probability of different numbers of clusters obtained in simulations for different values of the directional bias P. Other parameters are $R = 1$ and $\sigma = 0.02$. For any given parameter set, the probabilities were calculated based on one hundred simulation runs. Note that for these parameters the number of clusters less than three has never been observed.

No. of clusters	$P = 0.6$	$P = 0.7$	$P = 0.8$	$P = 0.9$	$P = 1$
3	0	0.01	0.01	0.01	0.02
4	0.51	0.56	0.48	0.42	0.42
5	0.45	0.4	0.47	0.52	0.5
6	0.04	0.03	0.04	0.05	0.06

Table 3: The probability for different numbers of clusters obtained in simulations for a different balance between the random and directional movement as quantifies by parameters σ and P, respectively. The perception radius is chosen as $R = 1$. For any given parameter set, the probabilities were calculated based on one hundred simulation runs. Note that the probabilities do not add up to one as in some simulations no stable clusters are formed (see also Fig. 8 and the comments in the text).

	$\sigma = 0.02$				$\sigma = 0.05$				$\sigma = 0.1$		
No. of clusters	3	4	5	6	2	3	4	5	2	3	4
$P = 0.52$	0.12	0 .72	0.05	0	0.12	0.19	0	0	0	0	0
$P = 0.55$	0.05	0.61	0.31	0	0	0.55	0.38	0	0.33	0.25	0
$P = 0.6$	0.1	0.42	0.43	0.05	0	0.23	0.71	0.04	0.07	0.73	0.13

number of clusters were counted, and for each number of clusters its frequency was calculated. The results are summarized in Tables 1–3. Whilst the dependence of the results on the perception radius is intuitive, i.e. the number of clusters tends to decrease with an increase in R (see Table 1, also cf. Fig. 1 obtained for $R = L = 10$), the dependence on P is not. It is readily seen from Table 2 that, even in the case $P = 1$ when the movement becomes 'more deterministic' (the animal always move along the population density gradient), the

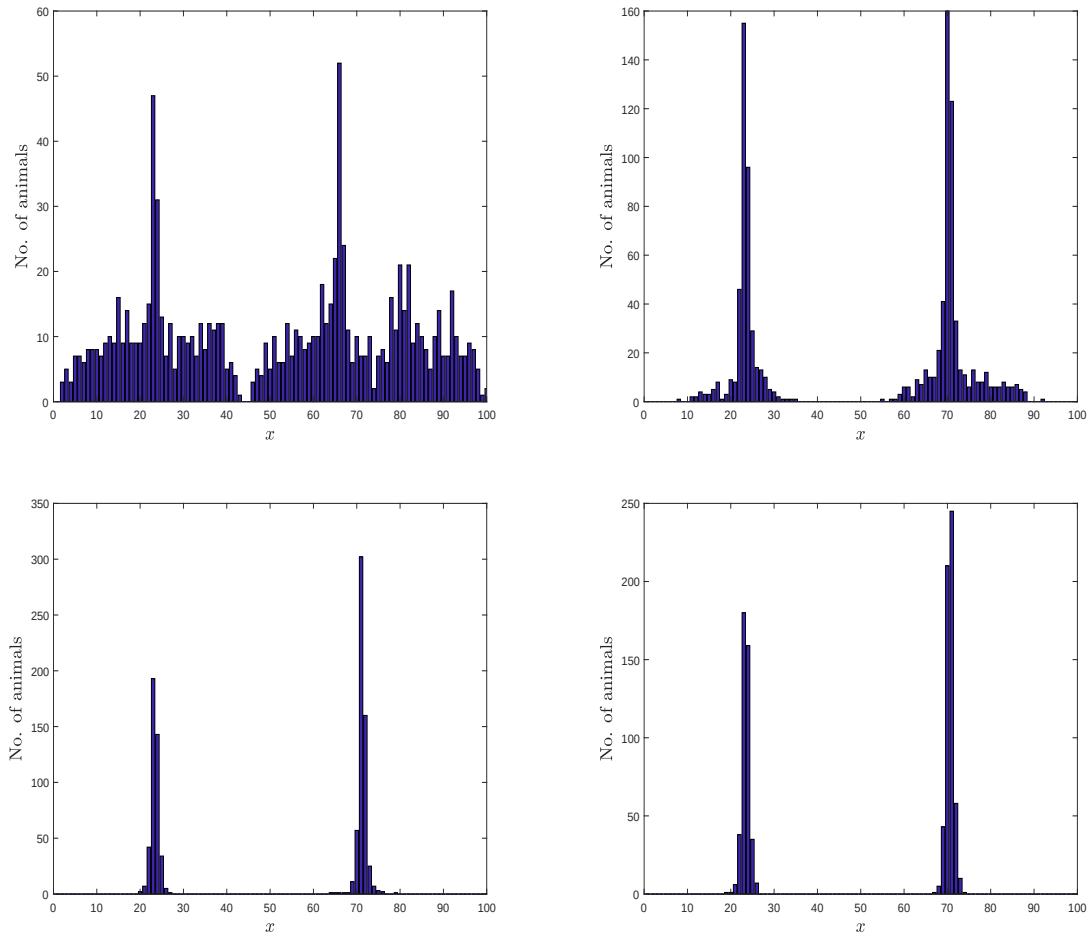

Figure 6: Population density over space obtained at different moments for the perception radius $R = 2$, other parameters are the same as in Fig. 3.

system retains its stochastic nature as the evolution of the initial conditions can still lead to a different number of clusters.

We also notice that, with an increase in σ, not only the number of clusters tends to decrease (cf. Table 3) but also their shape changes; in particular, they become less aggregated. A typical example is shown in Fig. 7. The effect of σ will be further investigated in Section 3.3.

Since parameter P quantifies the strength of the directional bias, one can expect that for the values of P close to 0.5 (where the bias disappears), the random component of the movement may be prevailing over the directional component and therefore clusters may become poorly defined or do not emerge at all. This is indeed what is observed in the simulations. Figure 8 shows the spatial population distribution at a large time ($t = 9000$) obtained for $P = 0.52$. It is readily seen that the population is now distributed over the space more uniformly than it was for larger values of P. Altogether, it leads to the conclusion that the formation of clearly defined clusters is a result of the directional density-dependent individual animal movement.

A question arises here as to how stable is the number of clusters in the course of time. We have addressed it by means of long-term simulations. We have observed that the system's

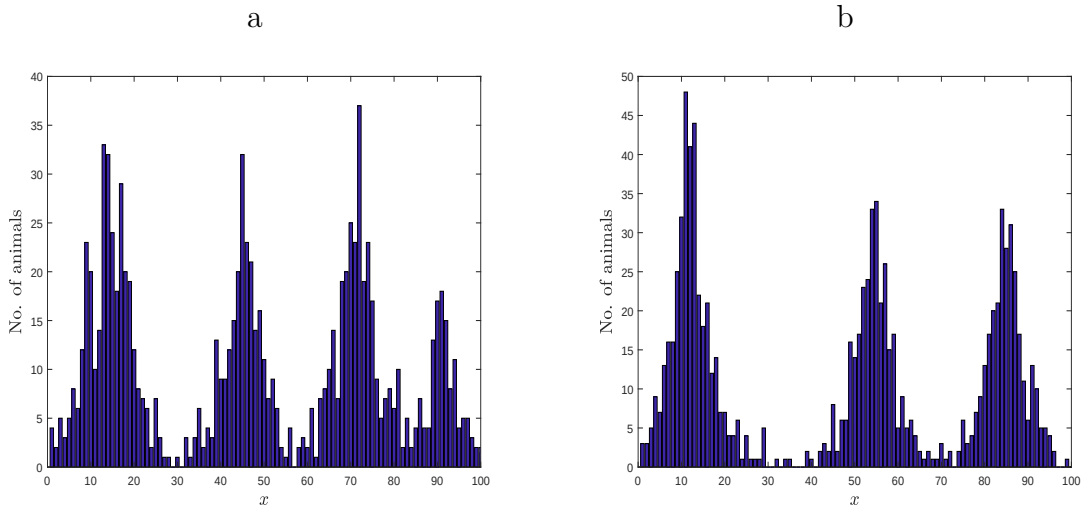

Figure 7: Population density over space at (a) $t = 100$ and (b) $t = 10000$ obtained for movement parameters $\sigma = 0.1414, P = 0.6$ and $R = 1$, other parameters are the same as above.

dynamics has two different time scales. For values of σ sufficiently small (e.g. $\sigma \leq 0.1$) and the values of P not too close to the critical value 0.5 (e.g. $P \geq 0.55$), clearly shaped clusters are formed by the time $t \sim 500$. Once emerged, this pattern can remain unchanged (subject to just small variations in the clusters size and width, cf. Fig. 4) over a considerable time, up to $t = 5000$ or even longer. However, this appears to be a transient state rather than an asymptotical one as the number of clusters then can change suddenly to another value. An example of this dynamics is shown in Fig. 9: over the first stage, the number of clusters in the pattern is five (cf. Fig. 5) but it suddenly changes to four at $t \approx 5000$. Once a new pattern with a different number of clusters emerges, it then remains unchanged; we did not observe any further changes in long-term simulations.

The dynamics becomes essentially different in case of either σ becoming sufficiently large or P sufficiently small. One example is shown in Fig. 10 where the number of clusters never

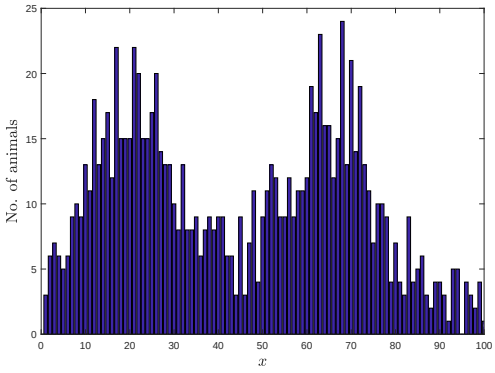

Figure 8: Population density over space obtained at $t = 9000$ for $P = 0.52$ and $\sigma = 0.1$, other parameters are the same as in Fig. 3.

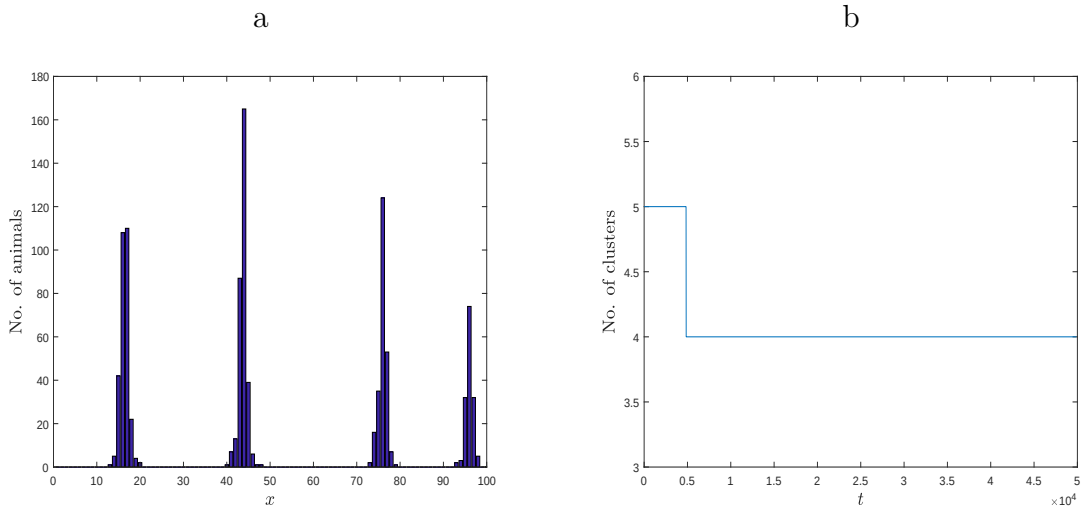

Figure 9: (a) Population density over space obtained at $t = 50000$ for $\sigma = 0.02$, $R = 1$ and $P = 0.6$, other parameters are the same as above; (b) the number of the clusters in the pattern vs time. Note the abrupt transition from five to four at $t \approx 5000$.

stabilizes. We will call this type of spatiotemporal pattern "dynamical clusters". Similarly to the previous case (cf. Fig. 9), the dynamics has a few different time scales corresponding to different stages of the dynamics. Over the first stage, the number of clusters fluctuates wildly (for the parameters of Fig. 10, between zero and four). At approximately $t = 2500$, the dynamics partially stabilizes by decreasing the range of fluctuations in the number of clusters between one and three. Another change occurs at $t \approx 12000$ when the fluctuations in the number of clusters occurs predominantly between one and two (occasionally jumping up to three). No further changes in the dynamics is observed at larger time.

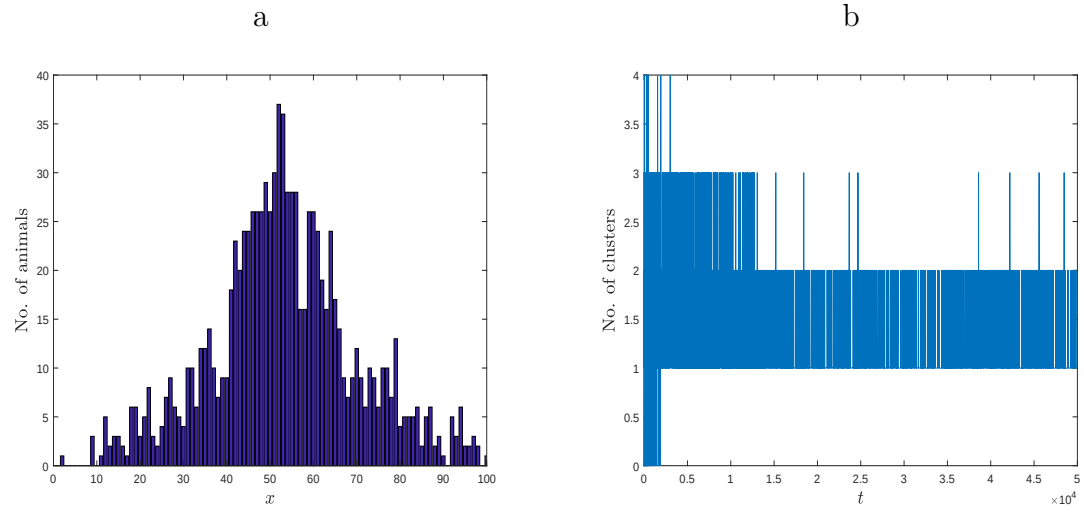

Figure 10: (a) Population density over space obtained at $t = 50000$, parameters are the same as in Fig. 8; (b) the number of the clusters in the pattern vs time.

3.2 Power law: Levy walkers

Now we are going to consider the case where the individual movement is described by a power law as in Eq. (3). In order to make a sensible comparison between the results obtained for the dispersal kernel given by the normal distribution (see the previous section) and those obtained for the power law (see below), a certain condition of equivalence must be established. For distribution with a finite variance, one way for doing that is to equalize the variance of different probability distributions. However, this approach does not work in the most interesting case of fat-tailed distributions, i.e. Eq. (3) with $1 < \gamma \leq 3$, because the dispersal kernel (3) does not have a finite variance then. We therefore use a different approach [6], namely, we equalize the survival probabilities, i.e. the probabilities for the moving animal to remain within a given domain over a given interval. Let x_t be the location of a given animal at a given time t, then the probability that at the next observation time $(t+1)$ the animal will remain within a given distance r of its previous location, i.e. $x_t - r < x_{t+1} < x_t + r$, is calculated as follows:

$$P\left(x_t - r < x_{t+1} < x_t + r\right) \;=\; \int_{-r}^{r} \rho(\xi) d\xi. \tag{6}$$

For the two probability distributions, see Eqs. (2) and (3), we obtain, respectively:

$$P\left(x_t - r < x_{t+1} < x_t + r\right) \;=\; \mathrm{erf}\left(\frac{r}{\sqrt{2\sigma^2}}\right), \tag{7}$$

and

$$P\left(x_t - r < x_{t+1} < x_t + r\right) \;=\; 1 - \frac{k^{\gamma-1}}{(k+r)^{\gamma-1}}. \tag{8}$$

Setting the the survival probability at a hypothetical value 0.9 and taking into account that $\mathrm{erf}^{-1}(0.9) = 1.16$, we solve Eqs. (7) and (8) for r and equate the results (since r is the same), thus arriving at the following relation between the parameters:

$$k \;=\; 1.16\sqrt{2\sigma^2}\left(10^{\frac{1}{\gamma-1}} - 1\right)^{-1}. \tag{9}$$

Therefore, for a given normal distribution with variance σ^2, parameter k of the 'equivalent' (in the sense explained above) power law distribution (3) is given by relation (9).

Our simulations show that, in the population of Levy walkers, the random-uniform initial condition evolves to an aggregated (patchy) population distribution, apparently similar to the case of normal distribution. Typical results are shown in Fig. 11. However, we readily observe that, apart from the generic property of the system to form spatial patterns, the population of Levy walkers exhibits different properties compared to the population of the Brownian walkers with the equivalent Gaussian kernel. In particular, clusters are now much wider and less regular in shape. Moreover, the number of clusters is not fixed any more, cf. the middle and the bottom panels in Fig. 11. A more detailed insight into the temporal dynamics (see Fig. 12) shows how the number of clusters fluctuates with time in an irregular manner. For the first period of $t \approx 25000$ of the system's dynamics, the number of clusters fluctuates between

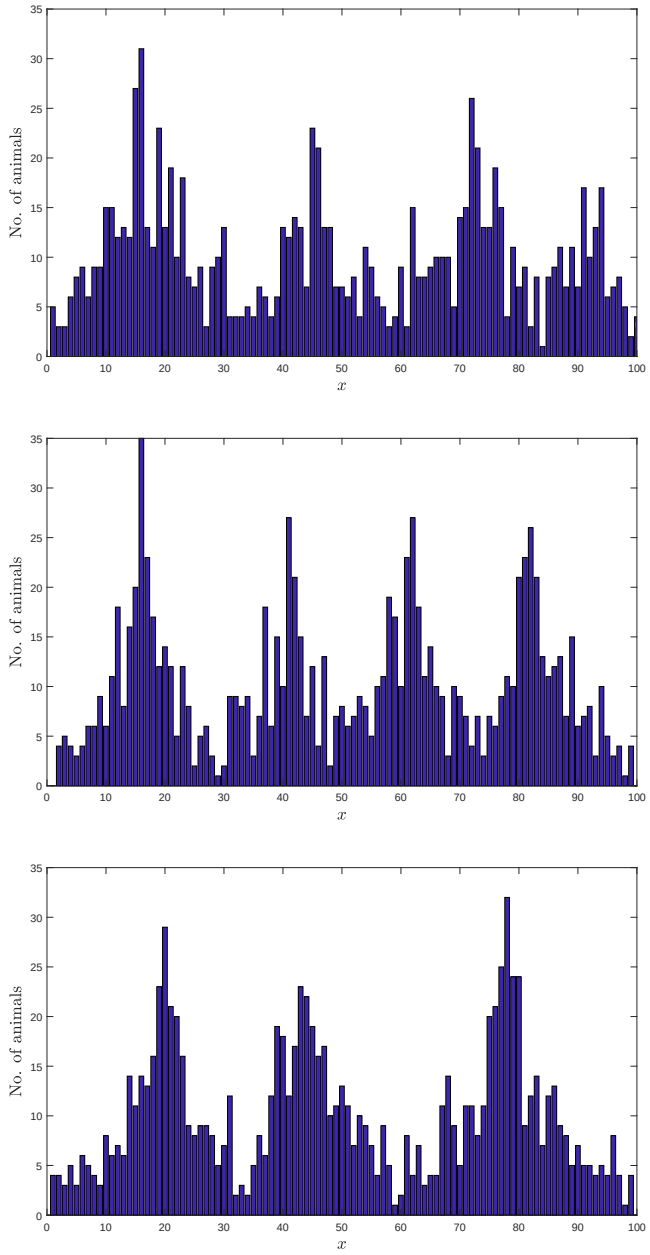

Figure 11: Clusters emerging in the population performing Levy flight (3) with $\gamma = 2$. Parameter $k = 0.0036$ is calculated using the equivalence condition (9) with $\sigma = 0.02$. Other parameters are $R = 1$ and $P = 0.6$, i.e. the same as in Fig. 3.

four and five. The system stays in the state with four clusters for most of the time (see the solid horizontal line in the left-hand side half of the figure) but makes short occasional excursion to the alternative state with five clusters. For convenience, we call this type of dynamics the "4/5-dynamics". Interestingly, the 4/5 dynamics is not sustainable and appears to be a very long transient. At $t \approx 25000$, the dynamics changes. Starting from $t \approx 25000$, the number of clusters fluctuates between three and four (being three for most of the time). We refer to this dynamics as "3/4-dynamics".

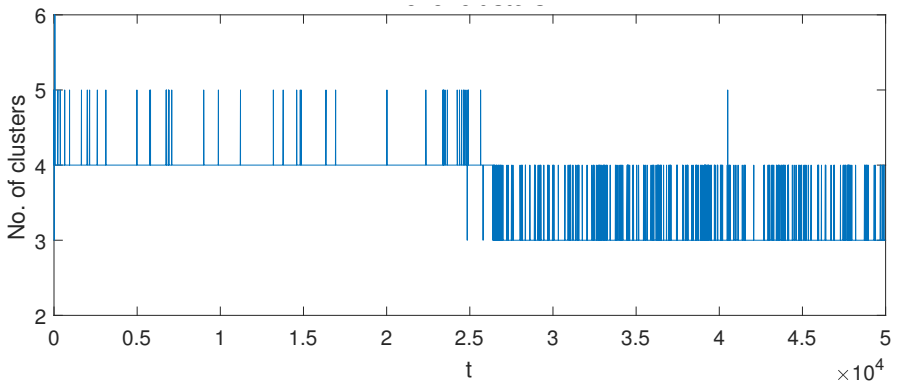

Figure 12: Number of clusters vs time, parameters are the same as in Fig. 11. Over the first 25000 units of time, the number fluctuates between four and five (4/5-dynamics), at later time the number fluctuates between three and four (3/4-dynamics).

We want to emphasize that the long term transient dynamics shown in Fig. 12 has nothing to do with the usual transients caused by the effect of the initial conditions. In order to demonstrate that, we describe the system's dynamics by the number of transitions between the states with different number of clusters (e.g. between four and five for $0 < t < 25000$) per one hundred time units. Figure 13 shows how this quantity changes with time. It is readily seen that the initial population distribution converges to the quasi-steady 4/5-dynamics by $t \approx 3000$. The system therefore exhibits two different time scales. The shorter time scale

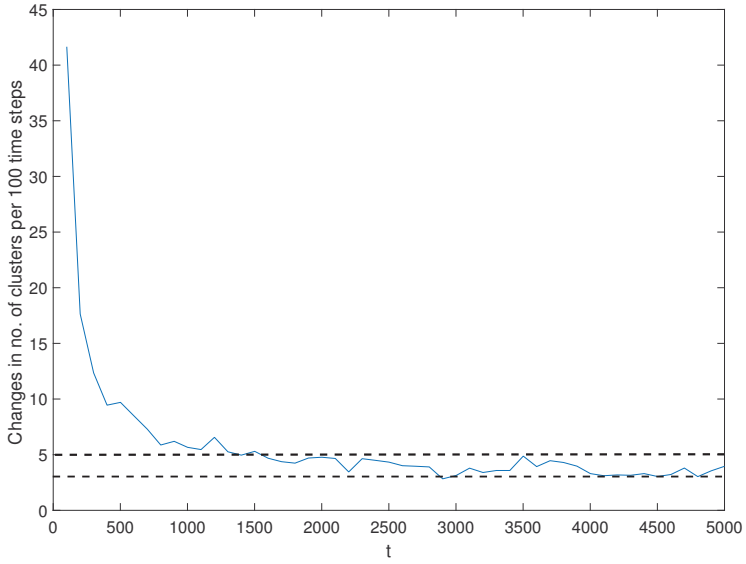

Figure 13: Average number of transitions per given time between the states with different number of clusters. Averaging was done over one hundred simulation runs. Parameters are the same as in Fig. 11. Convergence of the initial distribution to the quasi-steady "4/5-dynamics" is clearly seen as the number of transitions stabilizes within a certain range (as shown by the dashed horizontal lines) at $t \approx 1500$.

corresponds to the relaxation of the initial conditions to the 4/5 dynamics (Fig. 13), and the longer time-scale is the lifetime of the quasi-steady 4/5 dynamics before the system undergoes a fast transition to the asymptotical 3/4-dynamics at $t \approx 25000$.

Now we are going to check whether our results are sensitive to the value of threshold b which is a part of our definition of clusters. Whilst the results obtained for the equivalent population of Brownian walkers are not sensitive to the value of the threshold as the clusters are well defined (cf. Fig. 9), in the population of Levy walkers the clusters are volatile and the answer to the above question is by no means obvious. We therefore address this issue by analysing simulation results using different values of b. Results of the analysis are shown in Fig. 14. Note that here we use a simulation run different from that shown in Fig. 12, hence the results obtained for the same value $b = 0.02$ are similar but not identical, even though obtained for the same parameter values. It is readily seen that the number of clusters can become sensitive to the value of b when b becomes large. Remarkably, neither the existence of

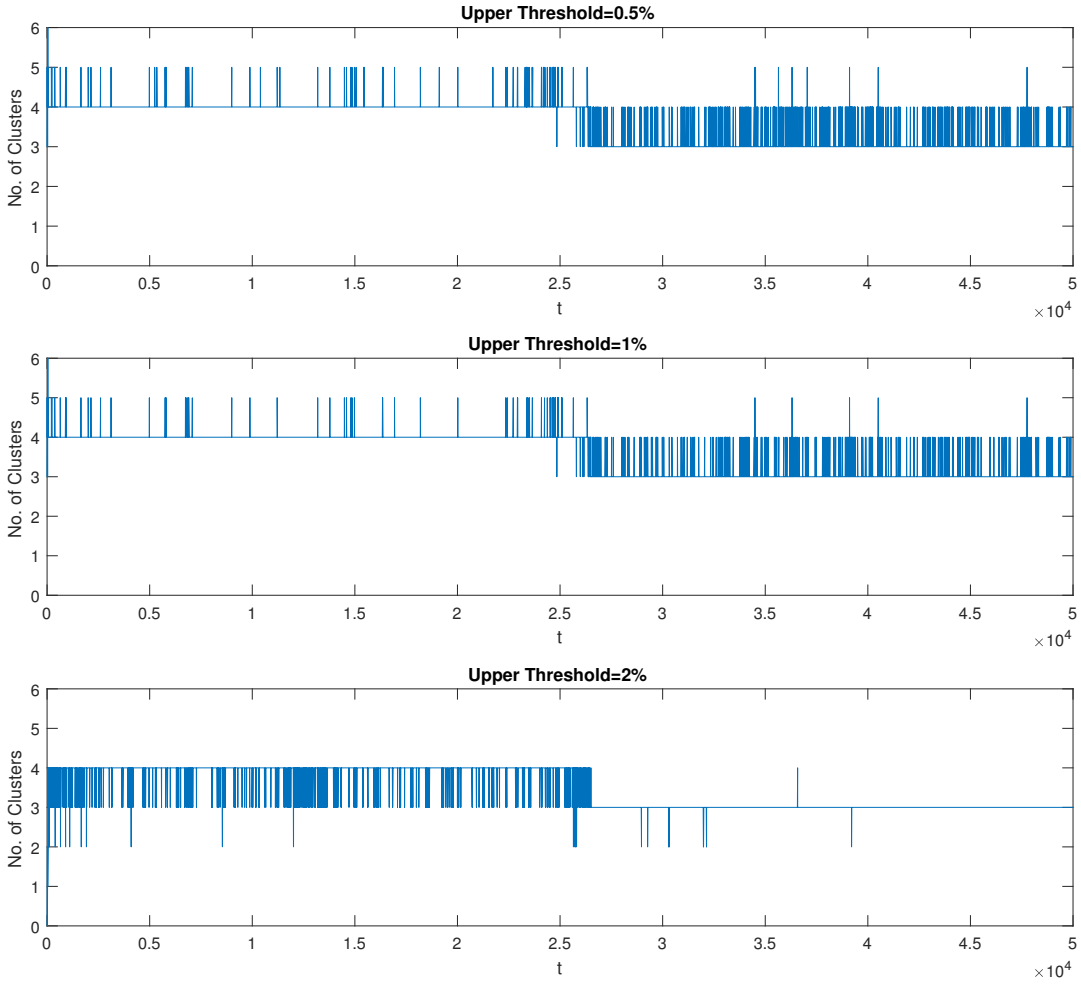

Figure 14: Sensitivity to the threshold density b defining cluster boundaries: number of clusters vs time for $b = 0.005$ (top), $b = 0.01$ (middle) and $b = 0.02$ (bottom). Parameters are the same as in Fig. 11.

dynamical clusters nor the existence of the long-term transient is sensitive to b. We therefore conclude that these are genuine properties of the population dynamics of Levy walkers.

We mention here that, due to the inherent stochasticity of the system, the duration of the long transient is essentially a random value. In our simulations, we observed that the timing of the transition to the asymptotical state can be anywhere between $t \sim 15000$ and $t \sim 45000$ (and occasionally taking smaller or larger values too). Also, in different simulations runs the 4/5 dynamics may include occasional excursions to the state with just three clusters, and the asymptotical state 3/4 may exhibit relatively frequent excursions to the state with five clusters.

An interesting question is how the properties of the system's dynamics may be different for different values of the exponent γ. Intuitively, one can expect that for sufficiently large values of γ the dynamics may become more similar to that of Brownian walkers, because power law distribution (3) with $\gamma > 3$ possesses a finite variance and hence converges to the normal distribution by the virtue of the Central Limit Theorem (although the convergence of power law to the normal distribution is slow). This is corroborated by simulations. Figure 15 shows the results obtained for $\gamma = 4$. It is readily seen that dynamical clusters do not exist in this case; the number of clusters do not fluctuate with time; see Fig. 15, right. Clusters themselves are well defined, similar to what was observed in the case of Brownian walkers, cf. Fig. 15 (left) and the bottom of Fig. 3. Interestingly, long term transient dynamics is observed also for $\gamma = 4$: the system does not converge to its final state of three clusters until $t = 10000$.

We have also checked the opposite case, i.e. very superdiffusive values $1 < \gamma < 2$; see the top row in Fig. 16. For comparison, the bottom row shows the case with $\gamma = 2$ (Fig. 16c) and $\gamma = 4$ (Fig. 16d). It is readily seen that for $\gamma = 1.1$ (Fig. 16a) there are no clusters, so that the population is spread all over the domain. As γ increases, areas of high population density becomes visible. For $\gamma = 1.5$ (Fig. 16b), the number of clusters fluctuates in time

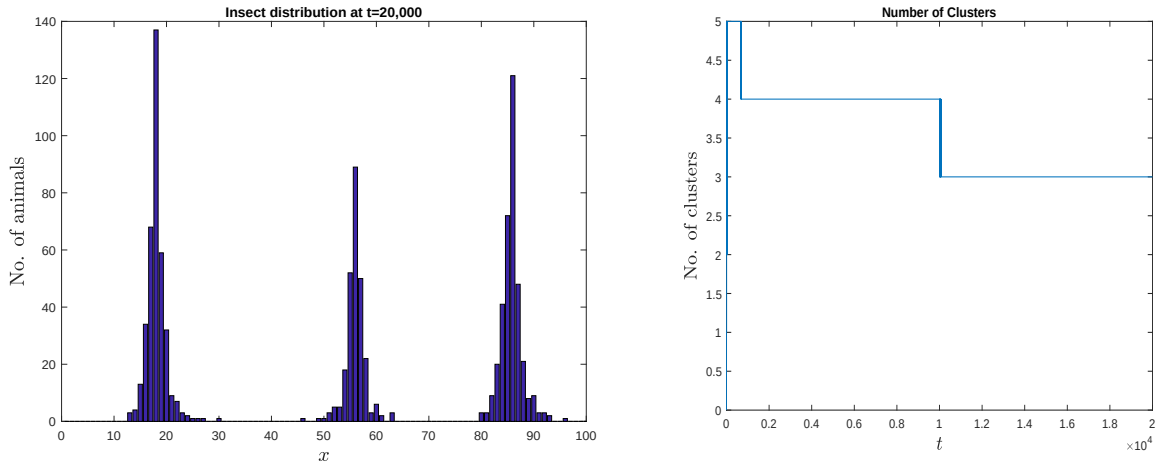

Figure 15: Population dynamics of animals performing the power law walk (3) with $\gamma = 4$: (left) spatial population distribution obtained at $t = 20000$, (right) number of clusters vs time. Parameters are the same as in Fig. 11.

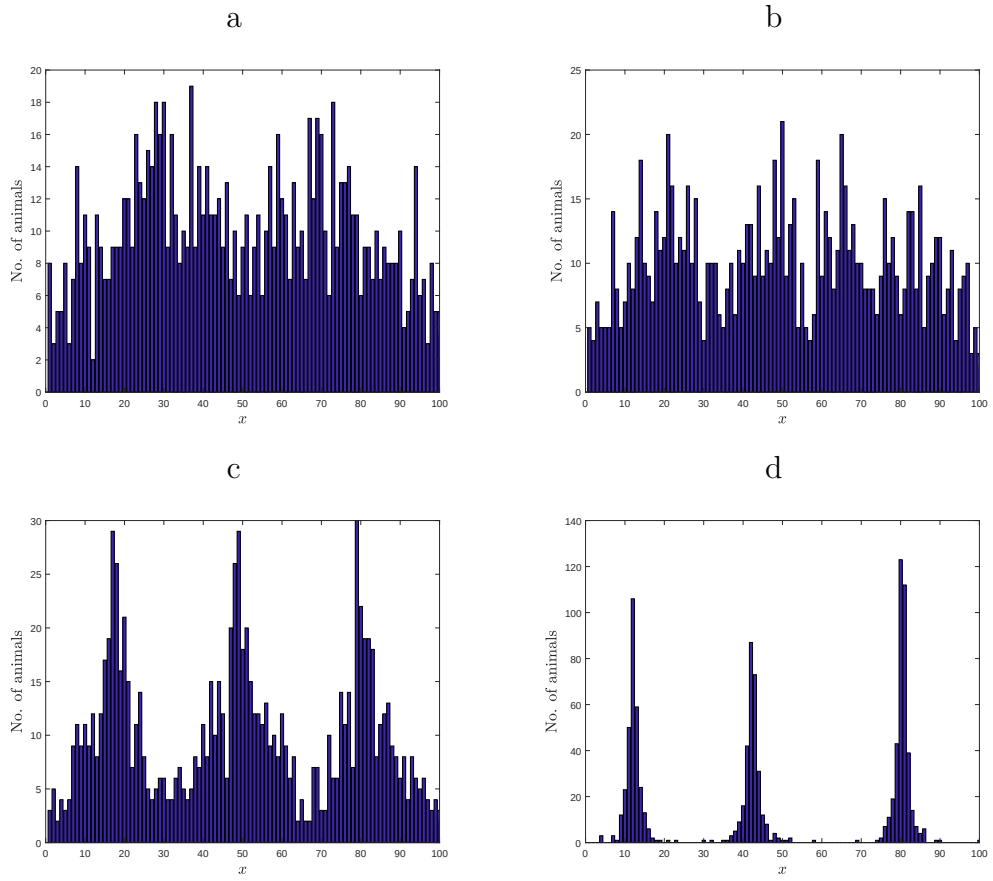

Figure 16: The distribution of animals for different values of γ. The corresponding values of parameter k are calculated from equating survival probabilities to that of the normal distribution with $\sigma = 0.02$. (a) $\gamma = 1.1$, (b) $\gamma = 1.5$, (c) $\gamma = 2$ and (d) $\gamma = 4$. All the distributions are shown at $t = 50000$. Parameters are the same as in Fig. 3.

from 0 to 3, the case of two clusters being most common (seen at approximately one half of the time steps). With a further increase in γ, clusters becomes clearly visible starting from $\gamma \approx 2$, these values they are dynamic and their number fluctuates with time (cf. Figs. 12 and 14). For $\gamma \geq 4$, clusters are well defined and stable; the population is strongly aggregated with high population density inside the clusters and approximately zero between the clusters.

3.3 Effect of the domain's finiteness

In the simulations above, we focused on the case of a large domain, i.e. where the characteristic movement step (as given by the value of the standard deviation σ of the normal distribution (2) or by the value of parameter k in case of the power-law distribution (3)) is much smaller than the size L of the domain, i.e. $\sigma/L \ll 1$ and $k/L \ll 1$. Arguably, in this case the effect of the domain boundedness is small and the animal movement mimics closely the corresponding movement in an unbounded space. A question arises here as to whether the significant

difference that we observed above between the properties of the spatial pattern emerging in the population of Brownian walkers and the population of Levy walkers would remain in case the effect of the domain boundedness becomes more prominent, i.e. when σ/L or k/L are not small any more.

Recall that in our model animals cannot leave the domain; see the second paragraph after Eq. (3). Effectively, it means that the tail of the distribution is cut off. Although this cutoff changes the asymptotical properties of the distribution (in particular, making the variance finite), in case $\sigma/L \ll 1$ or $k/L \ll 1$ the remaining part of the dispersal kernel that is actually used to generate movement steps is of significantly different shape. The different shape of dispersal kernels determines the difference in the emerging patterns.

However, the situation is different in the opposite case of a small domain, i.e. $\sigma/L \gg 1$ or $k/L \gg 1$. In this case, since the maximum value of the movement step $\Delta x \leq L$, $\Delta x/\sigma \ll 1$ and $\Delta x/k \ll 1$. Therefore, both the normal distribution and the power-law distribution can be well approximated by the first two terms in their Taylor expansion, that is

$$\rho\left(\Delta x\right) \approx \frac{1}{\sqrt{2\pi\sigma^2}}\left[1 - \frac{(\Delta x)^2}{2\sigma^2}\right] \qquad \text{and} \qquad \rho\left(\Delta x\right) \approx \frac{C}{k^\gamma}\left[1 - \left(\frac{|\Delta x|}{k}\right)^\gamma\right], \tag{10}$$

respectively. The functional form of the distributions therefore becomes similar (especially, in case $\gamma = 2$) and hence one can expect that the emerging patterns, if any, should have similar properties. In fact, any stable clusters are unlikely to appear at all: in a sufficiently small domain, both distributions are approximately constant (keeping only the first terms in Eqs. (10)), which means that the position of each animal at each movement step is drawn from a uniform probability distribution. Here we recall that this is the way how we generate the initial distribution (cf. Fig. 2). Therefore, in the case of a small domain (or large characteristic movement step), the animal movement is unlikely to result in the formation of clusters.

These heuristic arguments are confirmed by numerical simulations. Figure 17a shows the spatial distribution of the population density across the domain of length $L = 10$ obtained at $t = 3000$ for the normal distribution (2) with $\sigma = 50$; other parameters are the same as in Fig. 3. It is readily seen that there are no clusters; in fact, at any time $t > 0$ the distribution is not much different from the initial distribution (not shown here for the sake of brevity). The latter observation is confirmed by statistical measures: the variance of the initial population distribution and the distribution obtained at $t = 3000$ is 9.80 and 8.95, respectively. For comparison, Fig. 17b shows the spatial population distribution obtained at $t = 3000$ in simulations with the equivalent power-law kernel, i.e. Eq. (3) with $k = 9.114$, other parameters are the same. Similarly to the above, there are no clusters. The spatial distribution remains approximately uniform; the variance calculated for $t = 1$ (not shown) and $t = 3000$ (Fig. 17b) is 9.76 and 10.79, respectively. Note that these values are not much different from the values obtained in the case of normal distribution. We therefore conclude that, in case of a small domain, the population dynamics of Brownian walkers and Levy walkers are practically indistinguishable.

We have also checked how the results may change for a larger value of the perception radius R. For that, we performed simulations with $R = 10$ and other parameters the same

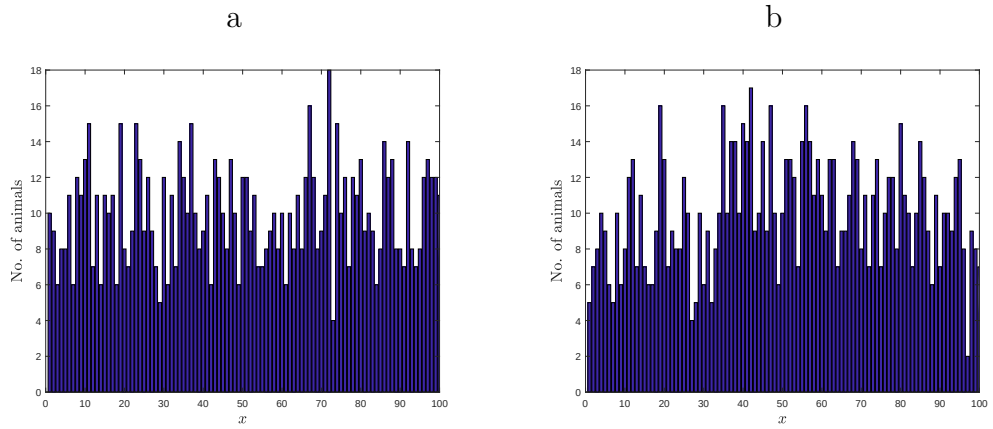

Figure 17: A histogram showing the population distributions at $t = 3000$ in the case of (a) the normal distribution of the movement steps obtained for $\sigma = 50$, other parameters are the same as in Fig. 3, and (b) the equivalent power law distribution. In both cases $R = 1$.

as in Fig. 17. The results that we obtained (not shown here for the sake of brevity) are very similar to the above. No clusters are formed and the population spatial distribution is approximately uniform across the domain.

We now notice that, even in the case of a large domain, e.g. for $\sigma/L \ll 1$ in the case of the normal distribution, the tail of the distribution never actually works, because the animal is not allowed to leave the domain. Similar observation obviously applies to the power law distribution, which means that its fat tail is in fact truncated. The truncated power law distribution has a finite variance, and that opens a possibility of using a different equivalence condition between the two dispersal kernels, namely by equating the variance. The question therefore arises as to how different the properties of the emerging spatiotemporal patterns obtained for the two movement types are going to be if they are compared in a different way – see below.

In order to address this issue, we perform the simulations as follows. Firstly, we consider the population dynamics of Levy walkers for parameters $\gamma = 2$, $k = 0.0036$, $R = 1$ and $P = 0.6$, i.e. as in Fig. 11. We pool together the movement step sizes made by all animals in the population ($N = 1000$) over the first ten thousand time steps. For the resulting data set of the movement steps (altogether, 10^7 random numbers), we calculate the variance to obtain the value $\sigma^2_{PLT} \approx 0.02$, so that the corresponding standard deviation is $\sigma_{PLT} \approx 0.1414$. We then simulate the dynamics of the population of the Brownian walkers subject to the new equivalence condition:

$$\sigma \;=\; \sigma_{PLT}, \tag{11}$$

keeping all other parameters the same as above. The results are shown in Fig. 18. It is readily seen that now the difference between the patterns emerging in the population of Levy walkers (Fig. 11) and in the equivalent population of Brownian walkers (as defined by (11)) is less drastic than it was previously (cf. Fig. 3). Yet the patterns remain clearly different; in particular, the population is much stronger aggregated and the clusters are more clearly

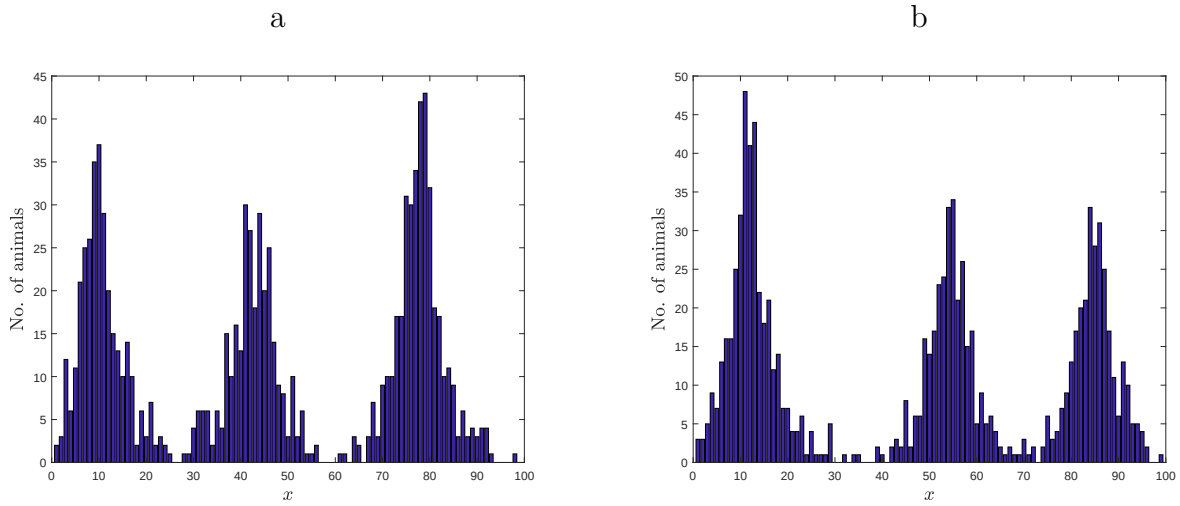

Figure 18: The distribution of insects across space obtained for $\sigma = 0.1414$ (other parameters are $R = 1$, $P = 0.6$, $N = 1000$ and $L = 10$, i.e. the same as in Fig. 3) and shown at (a) $t = 1000$ and (b) $t = 10000$.

shaped in the population of Brownian walkers. We therefore conclude that not only the large-distance asymptotics of the dispersal kernel but also its shape at intermediate distances plays an important role in shaping the population dynamics.

3.4 Statistical properties of the spatial patterns

3.4.1 Morisita index

As we have shown above, density-dependent individual movement normally results (for values of the variance not too large and the directional bias not too weak) in the formation of strongly heterogeneous spatial population distribution consisting of several clusters. Whilst this is clearly seen in the simulations results, the question is whether this self-organized heterogeneity could be described in a more quantitative way. There are several measures or indices that are used in statistical ecology for this purpose, e.g. see [29] for a short review. In particular, the Morisita index [54] has been widely used to quantify the heterogeneity of the spatial distribution [2, 26, 30]:

$$I_M = Q \frac{\sum_{k=1}^{Q} n_k(n_k - 1)}{N(N-1)}. \tag{12}$$

The Morisita index provides a measure of how likely it is that two randomly selected individuals in a given distribution are found within the same bin compared to that of a random distribution [54]. It can be proved that, if the individuals are distributed randomly (with a constant probability density) then I_M is close to one, and it is greater than one if the individuals are aggregated [34].

Using the definition (12), we have calculated I_M for several different spatial population distribution as given by Figs. 3, 8, 11 and 15. The results are shown in Table 3.4.1. Obviously,

Table 4: The Morisita index calculated for various spatial population distributions. N.D. and P.L. stand for the normal distribution and the power law distribution, respectively; see Eqs. (2–3).

	Sources	Dispersal kernel	Number of clusters	Morisita index, I_M
1	Fig. 3 ($t = 100$)	N.D.	4	1.817
2	Fig. 3 ($t = 200$)	N.D.	4	3.438
3	Fig. 3 ($t = 500$)	N.D	4	8.065
4	Fig. 3 ($t = 1000$)	N.D.	4	8.872
5	Fig. 8	N.D.	2	1.204
6	Fig. 11 ($t = 100$)	P.L. ($\gamma = 2$)	4	1.230
7	Fig. 11 ($t = 10000$)	P.L. ($\gamma = 2$)	4	1.352
8	Fig. 11 ($t = 30000$)	P.L. ($\gamma = 2$)	3	1.346
9	Fig. 15	P.L. ($\gamma = 4$)	3	7.120

the Morisita index is an adequate measure of the population aggregation: the conclusion as to which distribution is more aggregated based on the visual comparison appears to be in full agreement with I_M values. However, it is also readily seen that the Morisita index fails to distinguish between distribution with different number of clusters. For instance, the I_M value is close in the cases shown in rows 3 and 9 of the table; however, the number of clusters in the corresponding distributions is different. Similarly, the I_M value is approximately the same (up to the second digit) in rows 5 and 6, but the number of clusters is different. Also, the Morisita index is incapable of distinguishing between the different movement types: whilst rows 3 and 5 correspond to the Brownian walk, the distributions indexed in rows 6 and 9 are obtained for the power-law walk.

3.4.2 Sample frequency distributions

In the above, we have shown that different patterns of individual animal movement result in an emerging spatial population distribution with apparently different properties. The number of clusters, their size, shape, and their stability provide convenient theoretical measures to distinguish between the population distributions emerging in the populations of Browian and non-Brownian walkers. However, although providing useful information about the pattern as a whole, they hardly provide any information about the local population density (such as is given, in our approach, by the population size in any given bin). Meanwhile, considering the problem in a more practical perspective, it is the local information that ecologists normally obtain in empirical studies, e.g. through sampling. The number of samples collected in any given animal population census can vary quite significantly from, very rarely, being hundreds or even thousands of samples [1, 56, 83] to, rather typically, one or two dozen [7, 8] or, sometimes, a few or just one [5, 70]. Therefore, ecologists often have to operate with scarce spatial information that does not resolve details of the strongly heterogeneous population spatial distribution. As a result, the global properties of the distribution such as the location and the number of clusters (patches) remain obscure. An example is shown in Fig. 19a where red lines

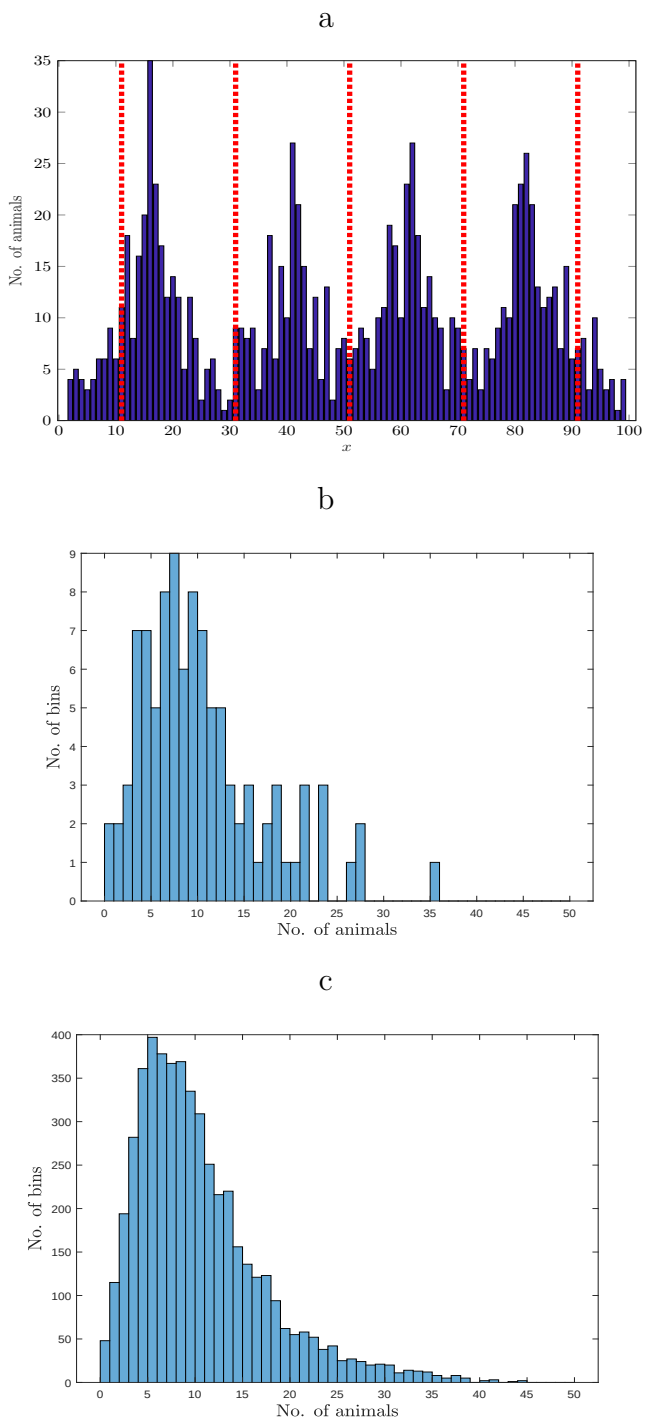

Figure 19: (a) Snapshot of the population spatial distribution obtained in the case of power law kernel (3) with $\gamma = 2$ and $k = 0.0036$ with other movement parameters as $R = 1$ and $P = 0.6$, vertical red lines indicates the hypothetical location where samples are taken. (b) Frequency distribution of sample values (all one hundred bins are used) obtained for the snapshot shown in (a). (c) Frequencies obtained from pooled multiple simulations, see details in the text; red curve shows the fitting of the data with a lognormal distribution, $R^2 = 0.996$.

indicate the location where the samples were collected and hence the population density (or its proxy, e.g. trap count) is known. Note that in this example none of the distribution maxima has been sampled. We therefore investigate whether differences between population distributions can be picked up and quantified based on local or spatially unstructured information such as an array of values of the population density for a given species (or their proxy, e.g. trap counts) collected on a sampling grid with no reference to population aggregation.

One way to analyse the sampling data, especially in the absence of knowledge of the spatial pattern, is to consider the frequency distribution of sample values. This approach was used in several empirical studies [7, 13, 15, 28, 74] and was shown to provide valuable insight into the properties of the corresponding population dynamics [62, 80]; see also [9, 94] for a more general framework. In order to demonstrate how to relate a given spatial pattern to the frequency distribution of sample values, let us consider the snapshot of the population distribution shown in Fig. 19a. We assume that the population sizes in different bins are statistically independent

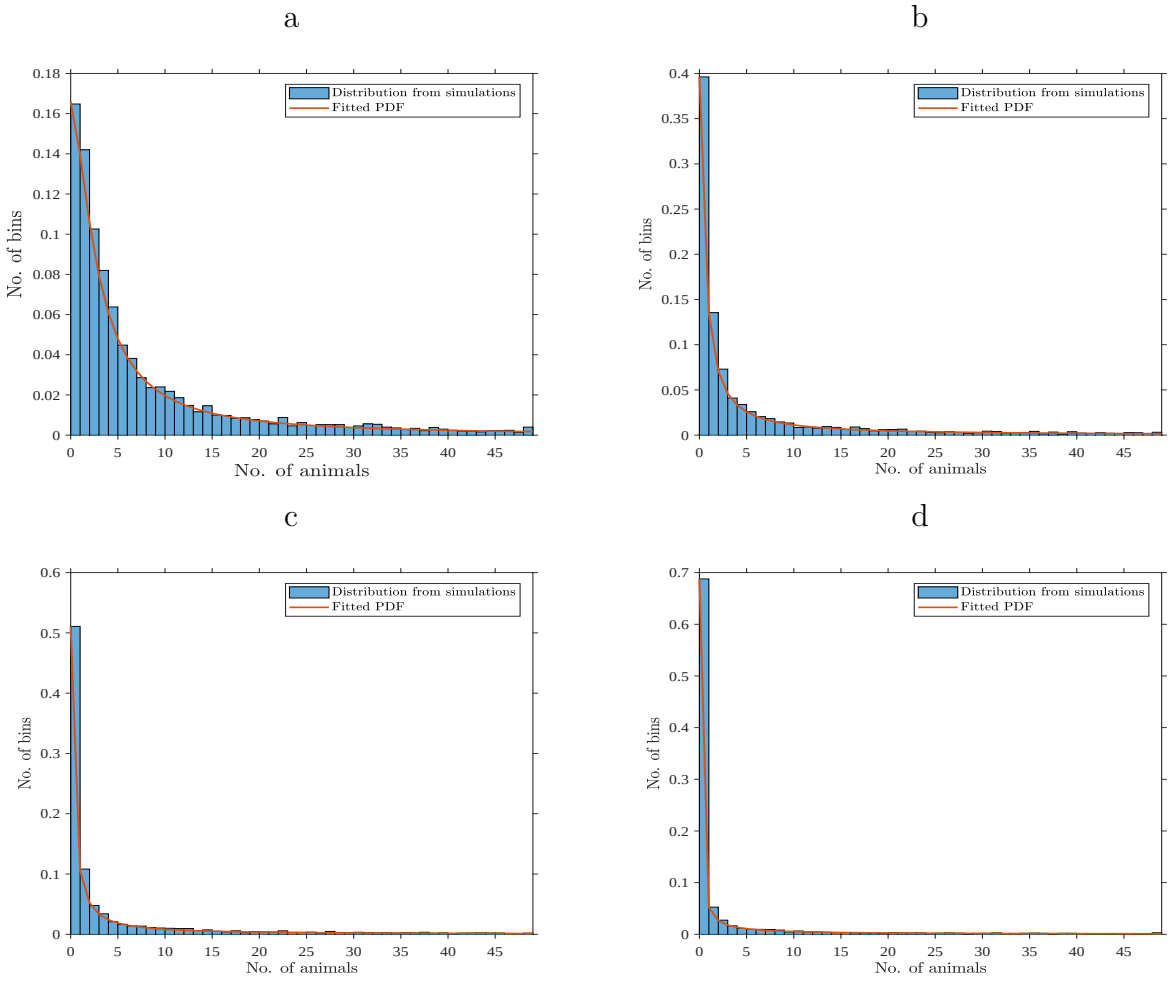

Figure 20: Frequency distribution of sample population density values obtained for the spatial population distributions simulated for different dispersal kernels: (a) power law (3) with $\gamma = 3$, (b) power law (3) with $\gamma = 4$, (c) power law (3) with $\gamma = 5$ and (d) normal distribution (2). Red curves show data fitting by a power law; see Table 5.

so that information obtained from all bins can be used, which gives an array of one hundred values of the population density. These numbers are arranged according to their frequencies resulting in the histogram shown in Fig. 19b. The obtained frequency distribution has a jagged, irregular shape, which indicates that one hundred values is not enough to produce a stable, sensible distribution of sample values. To obtain a histogram with a better defined shape, we therefore pool together results of multiple simulation runs. For the given parameter set, the simulations were repeated fifty times, thus producing altogether the pool of 5000 bin values that were then arranged into a histogram; see Fig. 19c. It is readily seen that the histogram of sample value frequencies now has a much smoother shape; in particular, it can be fitted very well by a lognormal distribution, cf. the red curve.

We now repeat the above procedure for different values of the power law exponent γ and for the normal distribution. Results are shown in Fig. 20. We readily observe that the properties of spatial population distributions (not shown here for the sake of brevity) emerging in the cases where individual movement is described by the power law (3) with $\gamma \geq 3$ is significantly different from the case $\gamma = 2$ which corresponds to Levy flights. Results obtained for larger values of γ are almost indistinguishable from the results obtained for the normal distribution, cf. Figs. 20c and 20d. All four frequency distributions shown in Fig. 20 can be fitted well by a power law, see Table 5 (note that the accuracy of the fitting increases with an increase in γ); however, it does not provide any sensible fitting for the sample value distribution obtained for $\gamma = 2$.

Table 5: Best-fit parameter values and R^2 values for the fitting of the sample frequency histograms shown in Fig. 20 by a power law $p(x) = c(h + x)^{-\mu}$.

	c	h	μ	R^2
$\gamma = 3$	$1.264 \cdot 10^6$	10.42	3.110	0.992
$\gamma = 4$	1578	0.8501	1.405	0.999
$\gamma = 5$	798.4	0.3977	1.261	1
Normal distribution	286.7	0.09068	1.035	1

4 Discussion and concluding remarks

Spatial distribution of ecological populations is often distinctly heterogeneous [18, 45, 44] and this is known to have profound implications for the population dynamics as well as for ecological monitoring and population management [16, 39, 64, 67, 75, 81, 90, 92, 93]. Whilst considerable progress has been done over the last two decades in the understanding of this phenomenon [45, 51, 52, 59], the effect of many relevant factors on the ecological pattern formation remains obscure and many questions yet wait to be answered, so that the problem remains to be a focus of research and discussion [65]. In particular, the role of individual movement behavior remains poorly understood, in spite of arguably being a key factor in

spatial ecology [10, 57]. Here we attempted to relate the problem of understanding of populations spatial patterning to another major focus in ecology, namely, to the effect of different individual movement patterns [68, 84, 89]. We have considered the spatial dynamics of a population where animals perform either Brownian or non-Brownian motion. In our simulation model, the individual movement is described by a dispersal kernel (probability distribution of travelled distances) which is parameterized, respectively, by the normal distribution or by a power law. Individual movement is modulated by density-dependence, so that an animal's advance towards areas with a higher population density is more likely.

Having performed intense computer simulations for movement parameters varying over a broad range, we have obtained the following results:

- Density-dependent individual movement results in the formation of animals clusters (patches of high population density), e.g. see Figs. 3, 5 and 11. The number of emerging clusters is a random variable, so that the population's aggregation properties are described by a probability distribution for a different number of clusters to appear (see Tables 1–3), not by a single number. The probability distribution (and hence the typical number of clusters) depends on the movement parameters such as the perception radius, the strength of density-dependence (directional bias) and the characteristic size of the movement step;

- In the case where the directional bias is sufficiently strong and the movement domain is large, the properties of the animals clusters differ significantly between the populations of Brownian walkers (dispersal kernel described by a normal distribution) and Levy walkers (power law kernel with the exponent $\gamma = 2$). Whilst in the population of Brownian walkers the number of clusters, once they have formed, does not change with time, in the equivalent population of Levy walkers the clusters are dynamical so that in the course of time the system experience fast transitions between the states with different number of clusters (see Figs. 11, 12 and 14). In case of the power law random walk with $\gamma > 3$, the emerging clusters are stable;

- The population dynamics of Levy walkers exhibits two different transient time scales. The shorter time scale t_{rel} is associated with the 'usual' relaxation of the initial conditions (see Fig. 13). However, the initial distribution converges to a quasi-steady state, not an asymptotic state. The other, much longer time scale $t_{LT} \gg t_{rel}$ is associated with the lifetime of the quasi-steady state. At time $t \sim t_{LT}$, the system experience a fast transition from the quasi-steady state to its asymptotic state (e.g. from the 4/5-dynamics to the 3/4-dynamics, see Fig. 12). The system's dynamics therefore exhibits long term transient behaviour (cf. [25]);

- The frequency distribution of local population density values ('samples') shows essentially different properties for the population of Levy walkers ($\gamma = 2$) and that of Brownian walkers. With an increase in γ, the frequency distribution experiences a gradual transformation, so that for larger values of γ it becomes virtually undistinguishable from the one obtained for the population of Brownian walkers (see Fig. 20).

In order to compare between the population dynamics of Brownian walkers and that of Levy walkers, we had to establish a certain condition of equivalence between the two different movement processes. We used a condition based on equating the survival probabilities; see Eqs. (7–9). A question may arise about the robustness of this criterium with regard to the spatial and temporal scales involved [3]. Also, the sensitivity of the results to the chosen value of the survival probability P_s is a matter of discussion ($P_s = 0.9$ in our simulations), i.e. how different the results could be for a different value of P_s. With regard to the latter, we notice that, the larger P_s is, the larger the part of the kernel is that is included into the calculation. For the kernels of different type, it means that the effect of their different shape is going to be greater for larger values of P_s. Therefore, an increase in P_s is likely to make the difference between the two movement processes even more significant. In the opposite situation when P_s is small, only the central part of the kernel is included, so that the difference between the Gaussian and the power law is insignificant, cf. Eqs. (10).

In this paper, we restricted our investigation to a hypothetical 1D case, i.e. the system with one spatial dimension. We want to emphasize that the 1D case is not at all abstract (in particular, it does not imply that animals live on a line): in terms of a more realistic 2D movement, the 1D system could correspond to either a narrow stripe or a transect across the movement area. Yet the question remains as to how different the system's dynamics may be if the movement is considered in a fully isotropic 2D case, i.e. without any constraints on the values of y-coordinate. Arguably, the answer depends on the strength of animal's behavioural response to meeting its conspecific. Especially in the case of movement in a narrow stripe, the animal's movement path would often pass very close to another animal. When movement occurs in the 2D space, such close encounters would happen much less frequently. In this paper, we assumed that the response is neutral, i.e. the animal keeps moving along its path without altering the movement direction or the movement step. In this case, the difference between the 1D and 2D cases is unlikely to be significant.

An obvious alternative to the above assumption is the case where the animal's response is not neutral, e.g. the moving animal would likely decide to stay close to its conspecific and hence to terminate its movement step. Terminating the movements step changes the asymptotics of the dispersal kernel by truncating its tail and hence diminishes the difference between Brownian and non-Brownian walkers. Since encounters would happens much less often in the 2D case than in the 1D case (and even less frequently in the 3D case), one can expect that the population dynamics would be significantly different in different spatial dimensions. In particular, one can expect that the difference between the Brownian and non-Brownian walkers will be more drastic in a higher dimensional space.

We also notice that in the case of Brownian walkers, assuming that the environment is isotropic, the 'full' 2D movement splits to a product of two 1D movements for x and for y, i.e. $\rho(\Delta\mathbf{r}) = \rho(\Delta x)\,\rho(\Delta y)$ where $\Delta\mathbf{r}$ is the movement step along the 2D path, $(\Delta\mathbf{r})^2 = (\Delta x)^2 + (\Delta y)^2$, and each of $\rho(\Delta x)$ and $\rho(\Delta y)$ is given by (2). Therefore, in the case of Brownian walkers an intuitive extension of our results onto the 2D case is straightforward; in particular, one can expect the emergence of animal clusters with the properties similar to those observed in our 1D simulations.

In the case of non-Brownian walkers, especially for $\gamma < 3$, extension of our results onto the 2D case is less straightforward. Although it seems intuitive that the main features of the population dynamics, such as the formation of clusters, should remain valid also in that case, it becomes difficult to make any prediction about the shape and spacing of the clusters. This requires a separate study and will become a focus of future work.

Our investigation is partially motivated by a recent study on the distribution and movement of grey slug *Deroceras reticulatum* in agricultural fields [20, 64]. Spatial distribution of slugs was shown to be remarkably patchy, with some of the patches being stable throughout the season but not necessarily between the seasons. Preliminary correlation analysis performed in the course of above study did not reveal any significant correlation between the distribution of slugs and the physical properties of soil [20]. Currently available information about movement pattern of individual slugs is meagre [19, 21, 24, 61] and does not allow for any conclusion about the movement pattern. There is, however, some empirical evidence that movement of slugs exhibits density-dependance as individual slugs respond to the presence of their conspecifics by following their trails [91], hence their movement along the gradient of the population density is more likely. The pattern formation scenarios reported in this paper can therefore be a plausible explanation of the slugs aggregation in agricultural fields, although currently available data does not allow for a quantitative comparison between theory and data. Further empirical research is therefore needed, in particular to reveal whether the individual slug movement can be classified into the Brownian or non-Brownian types and to quantify the strength of the density dependence.

Acknowledgements

All authors contributed equally to this work. Stimulating discussion of the problem with Keith F. A. Walters and Emily Forbes is appreciated. J.R.E. acknowledges support in the form of a Research Associateship from the School of Mathematics, University of Birmingham.

References

[1] Alexander, C.J.; Holland, J.M.; Winder, L.; Woolley, C.; Perry, J.N. (2005) Performance of sampling strategies in the presence of known spatial patterns. Ann. Appl. Biol. 146, 361-370.

[2] Amaral, M.K., Pellico Netto, S., Lingnau, C., Figueiredo Filho, A. (2015) Evaluation of the Morisita index for determination of the spatial distribution of species in a fragment of araucaria forest. Appl. Ecol. Environm. Res. 13(2): 361-372.

[3] Araújo HA, Raposo EP (2016) Lévy flights between absorbing boundaries: Revisiting the survival probability and the shift from the exponential to the Sparre-Andersen limit behavior. Phys. Rev. E 94, 032113.

[4] Barry C. Arnold (2015) Pareto Distributions (2nd Edition). Chapman and Hall / CRC.

[5] Baars MA, Van Dijk TS. 1984 Population dynamics of two carabid beetles at a Dutch heathland. I. Subpopulation fluctuations in relation to weather and dispersal. J. Anim. Ecol. 53, 375388.

[6] D. Bearup, C.M. Benefer, S.V. Petrovskii, R. Blackshaw. Revisiting Brownian motion as a description of animal movement: a comparison to experimental movement data. Methods in Ecology and Evolution, (2016), 7, 1525-1537.

[7] Bearup, D., Petrovskii, S.V., Blackshaw, R., Hastings, A. (2013) The impact of terrain and weather conditions on the metapopulation of Tipula paludosa in South-Western Scotland: linking pattern to process. *American Naturalist* **182**, 393-409.

[8] Boag B, Mackenzie K, McNicol JW Neilson R., 2010 Sampling for the New Zealand flatworm. In: Proceedings crop protection in Northern Britain 2010, p.4550.

[9] Bolker BM. 2008 Ecological models and data in R. Princeton, NJ: Princeton University Press.

[10] Bullock, J.M., Kenward, R.E., Hails, R.S. (Eds.), 2002. Dispersal Ecology. Blackwell, Oxford.

[11] Byers JA, 2000. Wind-aided dispersal of simulated bark beetles flying through forests. Ecol Model 125,231-243.

[12] Choi Y, Bohan D, Powers S, Wiltshire C, Glen D, Semenov M. 2004. Modelling Deroceras reticulatum (Gastropoda) population dynamics based on daily temperature and rainfall. Agriculture, Ecosystems and Environment 103:519525.

[13] Clarke-Harris D, Fleischer SJ. 2003 Sequential sampling and biorational chemistries for management of Lepidopteran pests of vegetable amaranth in the Caribbean. J. Econ. Entomol. 96, 798804.

[14] Codling, E.A., Plank, M.J., Benhamou, S. (2008) Random walk models in biology. Journal of the Royal Society Interface, 5, 813834.

[15] Damgaard C. 2009 On the distribution of plant abundance data. Ecol. Inform. 4, 7682

[16] Dunning, J.B., Stewart, D.J., Danielson, B.J., Noon, B.R., Root, T.L., Lamberson, R.H., Stevens, E.E. (1995) Spatially explicit population models: current forms and future uses. Ecological Applications 5, 3-11.

[17] D. Grüunbaum, A. Okubo (1994), Modelling social animal aggregations. In: Frontiers in Mathematical Biology. Lecture Notes in Biomathematics, Vol. 100, S.A. Levin, ed., Springer-Verlag, Berlin, pp. 296325.

[18] Grünbaum D. (2012) The logic of ecological patchiness. Interface Focus 2:150-155.

[19] Foltan P, Konvicka M, 2008. A new method for marking slugs by ultraviolet-fluorescent dye. J. Moll. Stud. (2008) 74, 293-297.

[20] Forbes E, Back M, Brooks A, Petrovskaya NB, Petrovskii SV, Pope T, Walters KFA (2017) Sustainable management of slugs in commercial fields: assessing the potential for targeting control measures. In: R.Hull, G.Jellis, M.May, P.Miller, S.Moss, C.Nicholls, J.Orson (eds.), Aspects of Applied Biology 134: 89–96.

[21] Grimm B, Paill W, Kaiser H., 2000. Daily activity of the pest slug *Arion lusitanicus* Mabille. J. Moll. Stud. 66, 125-130.

[22] Grimm, V., Railsback, S.F., 2005. Individual-based Modeling and Ecology. Princeton University Press, Princeton.

[23] S. Gueron, S.A. Levin, and D.I. Rubenstein (1996), The dynamics of herds: From individuals to aggregations, J. Theor. Biol. 182, 85-98.

[24] Hamilton PA, Wellingtom WG, 1981. The effects of food and density on the movement of *Arion alter* and Ariolimax columbianus (Pulmonata: stylommatophora) between habitats. Res. Popul. Ecol. 23, 299-308.

[25] Hastings A, Abbott KC, Cuddington K, Francis T, Gellner G, Lai YC, Morozov A, Petrovskii S, Scranton K & Zeeman ML. 2018. Transient phenomena in ecology. Science 361, eaat6412.

[26] Hayes, J.J., Castillo, O. (2017) A new approach for interpreting the Morisita index of aggregation through quadrat size. Int. J. Geo-Inf. 6, 296; doi:10.3390/ijgi6100296

[27] Heinsalu, E., Hernandez-Garcia, E., Lopez, C. (2010) Spatial clustering of interacting bugs: Lévy flights versus Gaussian jumps. Europhysics Letters, 92, 40011.

[28] Hengeveld R. 1979 The analysis of spatial patterns of some ground beetles (col. Carabidae). In Spatial and temporal analysis in ecology (eds M Cormack, JK Ord), pp. 333346. Fairland MD: International Co-operative Publishing House.

[29] Cang Hui, Ruan Veldtman and Melodie A. McGeoch (2010) Measures, perceptions and scaling patterns of aggregated species distributions. Ecography 33, 95-102.

[30] Hurlbert, S. (1990) Spatial distribution of the montane unicorn. OIKOS 58, 257271.

[31] de Jager, M., Bartumeus, F., Kolzsch, A., Weissing, F.J., Hengeveld, G.M., Nolet, B.A., Herman, P.M.J., de Koppel, J. (2014) How superdiffusion gets arrested: ecological encounters explain shift from Lévy to Brownian movement. Proceedings of the Royal Society B, 281, 20132605.

[32] Jansen, V.A.A., Lloyd, A.L., 2000. Local stability analysis of spatially homogeneous solutions of multi-patch systems. J. Math. Biol. 41, 232252.

[33] Jopp F, Reuter H, 2005. Dispersal of carabid beetles emergence of distribution patterns. Ecol Model 186, 389-405.

[34] Kanevski, M. (2004) Analysis and Modelling of Spatial Environmental Data. EPFL Press: Lausanne, Switzerland.

[35] Kareiva, P.M. (1983) Local movement in herbivorous insecta: applying a passive diffusion model to mark-recapture field experiments. Oecologia, 57, 322-327.

[36] Kareiva, P.M., Shigesada, N., 1983. Analyzing animal movement as a correlated random walk. Oecologia 56, 234238.

[37] Kawai, R., Petrovskii, S.V. (2012) Multi-scale properties of random walk models of animal movement: lessons from statistical inference. Proc. R. Soc. A 468, 1428-1451.

[38] Keller, E.F., Segel, L.A. (1970) Initiation of slime-mold aggregation viewed as an instability. J. Theor. Biol. 26, 399-415.

[39] Kelly, D. (1994) The evolutionary ecology of mast seeding. Trends in Ecology & Evolution. 9(12), 465470.

[40] Klausmeier, C. A. (1999). Regular and irregular patterns in semiarid vegetation. Science 284, 1826-1828.

[41] Kolokolnikov T, Carrillo JA, Bertozzi A, Fetecau R, Lewis M. (2013) Emergent behaviour in multi-particle systems with non-local interactions. Physica D 260, 1-4.

[42] Lefever, R. and O. Lejeune (1997). On the origin of tiger bush. Bull. Math. Biol. 59, 263-294.

[43] Levin, S., 1990. Physical and biological scales and the modelling of predator-prey interactions in large marine ecosystems. In: Sherman, K., Alexander, L., Gold, B. (Eds.), Large Marine Ecosystems: Patterns, Processes and Yields. AAAS, Washington, pp. 179187.

[44] Levin S. (1994) Patchiness in marine and terrestrial systems: from individuals to populations. Philos Trans R Soc B 343, 99103.

[45] S.A. Levin, T.M. Powell, and J.H. Steele, eds. (1993) Patch Dynamics. Lecture Notes in Biomathematics, Vol. 96. Springer-Verlag, Berlin.

[46] M.A. Lewis & S. Pacala (2000) Modeling and analysis of stochastic invasion processes. J. Math. Biol. 41: 387-429.

[47] Liebhold, A., W. D. Koenig, and O. N. Bjornstad. 2004. Spatial synchrony in population dynamics. Annual Review of Ecology, Evolution, and Systematics 35:467490.

[48] Liu Q.-X., et al. 2016. Phase separation driven by density-dependent movement: a novel mechanism for ecological patterns. Phys Life Rev 19, 107-21.

[49] Lomax, K. S. (1954). Business failures. Another example of the analysis of failure data. J. Amer. Stat. Assoc. 49: 847-52.

[50] Lyles, D., T. S. Rosenstock, A. Hastings, P. H. Brown. 2009. The role of large environmental noise in masting: general model and example from pistachio trees. Journal of Theoretical Biology 259: 701713.

[51] Malchow, H., Petrovskii, S.V., Venturino, E. (2008) *Spatiotemporal Patterns in Ecology and Epidemiology: Theory, Models, Simulations*, Chapman & Hall / CRC Press.

[52] Meron E. (2015) Nonlinear Physics of Ecosystems. CRC Press.

[53] Mogilner, A., Edelstein-Keshet, L., 1999. A non-local model for a swarm. J. Math. Biol. 38, 534-570.

[54] Morisita, M. (1959) Measuring of the Dispersion of individuals and analysis of the distributional patterns. Mem. Fac. Sci. Kyushu Univ. Ser. E 3, 65-80.

[55] Morozov, A.Y., Petrovskii, S.V. (2009) Excitable population dynamics, biological control failure, and spatiotemporal pattern formation in a model ecosystem. *Bulletin of Mathematical Biology* **71**, 863-887.

[56] Murchie, A.K., Harrison, A.J., 2004. Mark-recappture of New Zealand flatworms in grassland in Nothern Ireland. In Proceedings of the Crop Protection in Nothern Britain, Dundee, Scotland, 2526 February 2004; pp. 6367.

[57] Nathan, R., Getz, W. M., Revilla, E., Holyoak, M., Kadmon, R., Saltz, D. & Smouse, P. E. 2008 A movement ecology paradigm for unifying organismal movement research. Proc. Natl Acad. Sci. USA 105, 19 05219 059.

[58] Okubo, A. (1986). Dynamical aspects of animal grouping: Swarms, schools, flocks, and herds. Adv. Biophys. 22, 1-94.

[59] Okubo, A. and S. Levin (2001). Diffusion and ecological problems: Modern perspectives. Interdisciplinary Applied Mathematics, Vol. 14. Springer.

[60] Pareto V (1965) La Courbe de la Repartition de la Richesse (Originally published in 1896). In: Busino G, editor. Oevres Completes de Vilfredo Pareto. Geneva: Librairie Droz. pp. 1-5.

[61] Pearson AK, Pearson OP, Ralph PL, 2006. Growth and Activity Patterns in a Backyard Population of the Banana Slug, Ariolimax columbianus. The Veliger 48(3), 143-150.

[62] Petrovskaya, N.B., Petrovskii, S.V. (2017) Catching ghosts with a coarse net: use and abuse of spatial sampling data in detecting synchronization. *J. R. Soc. Interface* **14**, 20160855.

[63] Petrovskaya N.B., Petrovskii S.V, Murchie A.K., 2012. Challenges of ecological monitoring: estimating population abundance from sparse trap counts. J R Soc Interface 9, 42035.

[64] Petrovskaya, N.B., Forbes, E., Petrovskii, S.V., Walters, K.F.A. (2018) Towards the development of a more accurate monitoring procedure for invertebrate populations, in the presence of unknown spatial pattern of population distribution in the field. Insects 9, 29; doi:10.3390/insects9010029

[65] Petrovskii, S.V. (2016) Pattern, process, scale, and models sensitivity. *Physics of Life Reviews* **19**, 131-134.

[66] Petrovskii, S.V., Li, B.-L., Malchow, H. (2004) Transition to spatiotemporal chaos can resolve the paradox of enrichment. *Ecological Complexity* **1**, 37-47.

[67] S.V. Petrovskii, N.B. Petrovskaya & D. Bearup (2014) Multiscale approach to pest insect monitoring: random walks, pattern formation, synchronization, and networks. Physics of Life Reviews 11: 467-525.

[68] Pyke, G.H. (2015) Understanding movements of organisms: its time to abandon the Levy foraging hypothesis. Methods in Ecology and Evolution, 6, 1116.

[69] C. Pioua, U. Berger, H. Hildenbrandt, V. Grimm, K. Diele, and C. D'Lima, 2007. Simulating cryptic movements of a mangrove crab: Recovery phenomena after small scale fishery. Ecological modelling, 205, 110-122.

[70] Raimondo S, Liebhold AM, Strazanac JS, Butler L. 2004 Population synchrony within and among Lepidoptera species in relation to weather, phylogeny, and larval phenology. Environ. Entomol. 29, 96105.

[71] Reynolds, A.M., Smith, A.D., Menzel, R., Greggers, U., Reynolds, D.R., Riley, J.R. (2007) Displaced honey bees perform optimal scale-free search flights. Ecology 88, 1955-1961.

[72] L.A.D. Rodrigues, D.C.Mistro, E.R.Cara, N.B.Petrovskaya, S.V.Petrovskii. (2015) Patchy invasion of stage-structured alien species with short-distance and long-distance dispersal. Bulletin of Mathematical Biology, 77:1583-1619.

[73] Rosenstock, T. S., A. Hastings, W. D. Koenig, D. J. Lyles, and P. H. Brown. 2011. Testing Morans theorem in an agroecosystem. Oikos 120:14341440.

[74] Rossi RE, Mulla DJ, Journel AG, Franz EH. 1992 Geostatistical tools for modeling and interpreting ecological spatial dependence. Ecol. Monogr. 62, 277314.

[75] Satake A., Iwasa Y,. (2000) Pollen coupling of forest trees: forming synchronized and periodic reproduction out of chaos. J Theor Biol. 203(2), 63-84.

[76] Segel, L.A., Jackson, J.L., 1972. Dissipative structure: An explanation and an ecological example. J. Theor. Biol. 37, 545-559.

[77] Skellam, J.G. (1951) Random dispersal in theoretical populations. Biometrika 38(12), 196-218.

[78] O.J. Schmitz and G. Booth, 1997. Modelling food web complexity: The consequences of individual-based, spatially explicit behavioural ecology on trophic interactions. Evolutionary Ecology 11, 379-398.

[79] Sims, D.W., Southall, E.J., Humphries, N.E., Hays, G.C., Bradshaw, C.J.A., Pitchford, J.W. et al. (2008) Scaling laws of marine predator search behaviour. Nature 451, 10981102.

[80] Sun J, Cornelius SP, Janssen J, Gray KA, Motter AE. 2015 Regularity underlies erratic population abundances in marine ecosystems. J. R. Soc. Interface 12, 20150235.

[81] Swetnam, T.W., Lynch, A.M. (1993) Multicentury, regional-scale patterns of Western spruce budworm outbreaks. Ecological Monographs 63, 399-424.

[82] Thomas CFG, Parkinson L, Marshall EJP. (1998) Isolating the components of activity-density for the carabid beetle Pterostichusme lanarius in farmland. Oecologia 116:103-112.

[83] Tobin, P.C., Blackburn, L.M., Gray, R.H., Lettau, C.T., Liebhold, A.M., Raffa, K.F., 2013. Using delimiting surveys to characterize the spatiotemporal dynamics facilitates the management of an invasive non-native insect. Popul Ecol 55:545555

[84] Turchin, P. (1998) Quantitative analysis of movement. Sunderland, Sinauer.

[85] Tyutyunov, Y.V, Senina, I., Arditi, R., 2004. Clustering due to acceleration in the response to population gradient: a simple self-organization model. Am. Nat. 164 (6), 722-735.

[86] Tyutyunov, Y.V., Zagrebneva, A.D., Surkov, F.A., Azovsky, A.I., 2009. Microscale patchiness of the distribution of copepods (Harpacticoida) as a result of trophotaxis. Biophysics 54 (3), 508-514.

[87] van de Koppel J, Gascoigne JC, Theraulaz G, Rietkerk M, Mooij WM, Herman PMJ. (2008) Experimental evidence for spatial self-organization and its emergent effects in mussel bed ecosystems. Science 322:73942.

[88] Viswanathan, G.M., Afanasyev, V., Buldyrev, S.V., Murphy, E.J., Prince, P.A., Stanley H.E. (1996) Levy flight search patterns of wandering albatrosses. Nature 381, 413415.

[89] Viswanathan, G.M., da Luz, M.G.E., Raposo, E.P., Stanley, H.E. (2011) The physics of foraging: an introduction to random searches and biological encounters. Cambridge University Press, Cambridge.

[90] Wallin, H. (1988) The effects of spatial distribution on the development and reproduction of Pterostichus cupreus L., P. melanarius Ill., P. niger Schall. and Harpalus rufipes DeGeer (Col., Carabidae) on arable land. J. Appl. Entomol. 106, 483-487.

[91] Wareing DR (1986) Directional trail following in Deroceras reticulatum (Muller). J. Moll. Stud. 52, 256-258.

[92] Williams JC, ReVelle CS, Levin SA (2005) Spatial attributes and reserve design models: a review. Envir. Mod. Assess. 10, 163-181.

[93] Wu JG, Loucks OL (1995) From balance of nature to hierarchical patch dynamics: A paradigm shift in ecology. Quart. Rev. Biol. 70, 439-466.

[94] Young LJ, Young J. 1998 Statistical ecology. Berlin, Germany: Springer.